

Water Resources Research®

RESEARCH ARTICLE

10.1029/2021WR030480

Key Points:

- First broad characterization of large-flood occurrence in the conterminous United States in the modern hydroclimate, including seasonality
- Both traditional and novel methods to assess temporal distribution of large floods
- Few significant temporal trends, but significant relations to climate indices for some regions and seasons

Supporting Information:

Supporting Information may be found in the online version of this article.

Correspondence to:

M. J. Collins,
mathias.collins@noaa.gov

Citation:





Collins, M. J., Hodgkins, G. A., Archfield, S. A., & Hirsch, R. M. (2022). The occurrence of large floods in the United States in the modern hydroclimate regime: Seasonality, trends, and large-scale climate associations. *Water Resources Research*, 58, e2021WR030480. <https://doi.org/10.1029/2021WR030480>

Received 28 MAY 2021

Accepted 29 JAN 2022

Published 2022. This article is a U.S. Government work and is in the public domain in the USA.

The Occurrence of Large Floods in the United States in the Modern Hydroclimate Regime: Seasonality, Trends, and Large-Scale Climate Associations

M. J. Collins¹ , G. A. Hodgkins² , S. A. Archfield³ , and R. M. Hirsch³ 

¹National Marine Fisheries Service, National Oceanic and Atmospheric Administration, Gloucester, MA, USA, ²U.S. Geological Survey, New England Water Science Center, Augusta, ME, USA, ³U.S. Geological Survey, Water Resources Mission Area, Reston, VA, USA

Abstract Many studies investigate river floods by analyzing annual maximum series that record the largest flow of each year, including many within-bank events inconsequential for human communities. Fewer focus on larger floods, especially at the continental scale. Using 473 streamgages across the conterminous United States with near-natural flow from 1966 to 2015, we characterized the seasonality, occurrence, and climatic associations of the 10 largest and 2 largest floods at each site. These are often overbank events that have ecosystem functions and pose risks to humans. We grouped sites into 14 clusters corresponding to climatic and physiographic regions and characterized their flood seasonality at a monthly resolution using a probabilistic method. We then evaluated annual occurrence regionally and nationally, and seasonal occurrence regionally, by complementing a traditional approach to trend analyses with a novel method based on expected occurrence. Relationships between flood occurrence and climate indices were also investigated. Large floods have strong seasonality in some regions, but in areas with numerous flood-generating mechanisms, seasonality is more complex. There is little evidence nationally that large riverine floods are more or less frequent than expected in recent years and only two regions show significant trends in annual counts; few show seasonal trends. We found some regional relationships between flood counts and climate indices, annually and seasonally; nationally the Pacific North American pattern is related to annual counts of the 2 largest floods. Large-flood occurrence was generally stable across the United States in the last five decades; this may or may not continue with projected warming.

Plain Language Summary Flood studies usually focus on records of the largest streamflow of each year because they are widely available and provide relatively large samples. However, the largest flow of each year is not necessarily big enough to inundate the floodplain and pose risks to human communities. Our study investigated only the largest observed floods in the record, ones that occur roughly every five to fifty years. We used a set of 473 gages that measure near-natural river flow across the United States. We studied many aspects of these consequential events at regional and national scales for the period 1966–2015, including seasonality, changes over time, and associations with known climate patterns. We found that the seasonality of large floods is strong in some regions, but weak or complex in others where floods have a variety of causes. There is little evidence that large floods have become more or less frequent with time, but we found some regional and national associations between large-flood occurrence and known climate patterns such as the Pacific North American pattern. Large-flood occurrence has generally been stable in the last five decades, but continued re-evaluation of the historical record is important as new data are collected.

1. Introduction

River floods that overflow streambanks are natural phenomena that have a variety of impacts on floodplain ecosystems and human communities. Many are beneficial: for example, overbank floods are necessary for specific life stages of some species and periodic floodplain inundation is necessary for important sediment, organic matter, and nutrient exchanges in river-floodplain ecosystems (Junk et al., 1989; Lytle & Poff, 2004; Poff et al., 1997). However, overbank floods can also damage property and infrastructure and threaten lives (Ashley & Ashley, 2008; NOAA NCEI, 2021; Smith & Katz, 2013). To protect life and property, communities often make estimates of the likelihood and severity of future overbank floods and they frequently use historical records of streamflow in their community to do so (England et al., 2019). The most commonly used records, called “annual

maximum series (AMS)", record the largest instantaneous streamflow of the year for each year of record at a station. Flood magnitude and frequency estimates based on these records are then used for a variety of purposes, such as to design floodplain infrastructure and locate development outside of floodplains.

Because of their importance for design and planning, many U.S. flood studies analyze AMS records. They are also the most easily available, quality-assured flood records that provide coverage for thousands of streams in the United States (U.S. Geological Survey, 2020). AMS records are frequently the basis of flood studies in other parts of the world as well, although some investigations in the United States and elsewhere analyze records that include all peaks over a specified magnitude (i.e., peaks-over-threshold, or POT) where the threshold is often chosen so that an average of 2 or 3 events per year are analyzed. As described below, time series of rare events can also be identified by this approach.

Flood seasonality studies of the conterminous United States (CONUS) and globally most often focus on AMS floods (Blöschl et al., 2017; Burn & Whitfield, 2016; Lins & Slack, 2005; Villarini, 2016; Wasko et al., 2020; Ye et al., 2017). AMS records are also frequently used for analyzing historical trends and/or change points in flood magnitude (e.g., Ahn & Palmer, 2016; Blöschl et al., 2019; Burn & Whitfield, 2016; Douglas et al., 2000; Hodgkins et al., 2019; Lins & Slack, 1999; Ryberg et al., 2020; Villarini et al., 2009; Vogel et al., 2011), while POT series with more than one event per year are used to assess event frequency trends (e.g., Archfield et al., 2016; Armstrong et al., 2014; Burn et al., 2016; Hodgkins et al., 2019; Mallakpour & Villarini, 2015; Petrow & Merz, 2009). As with flood seasonality and trend studies, investigations of linkages between flood occurrence and various climate indices like El Niño-Southern Oscillation (ENSO) or the North Atlantic Oscillation (NAO)—sometimes called "teleconnection patterns"—typically focus on AMS or POT floods (e.g., Archfield et al., 2016; Armstrong et al., 2014; Dickinson et al., 2019; Mallakpour & Villarini, 2016; Pizarro & Lall, 2002; Villarini et al., 2012).

Despite their widespread use, AMS flood series (and POT series with >1 event per year) have limited utility for characterizing large, overbank floods—their seasonality, changes over time, and large-scale climate linkages—because these events occur, on average, less frequently than every year or two in alluvial channels (Wolman & Miller, 1960). AMS records include many small floods that remain within the channel and thus are not very consequential for human communities.

We define large floods in this study as the 10 largest AMS floods observed in a 50 yr period from 1966 to 2015. These instantaneous flood peaks have empirical recurrence intervals ranging from approximately 5 yr (10th largest event) to 50 yr (largest event) for this record length. These are frequently overbank floods at a given site and, therefore, the river floods that cause the most concern for loss of property and life.

Studies targeting large floods in CONUS have often had a narrow focus on hydrometeorologic analyses of specific events (e.g., Smith & Baeck, 2015; Smith et al., 2019, 2018) and/or small geographic areas (e.g., Agel et al., 2019), or developing envelope curves to understand the maximum unit discharges that can be generated by meteorological events (Costa, 1987; Crippen & Bue, 1977; O'Connor & Costa, 2004). Few have investigated historical trends in large floods across CONUS (Dethier et al., 2020; Hodgkins et al., 2017; Milly et al., 2002; Slater et al., 2021; Wasko et al., 2021), fewer yet have studied large-flood teleconnection patterns (Hodgkins et al., 2017; Villarini et al., 2014), and to our knowledge none have focused on large-flood seasonality. Yet, studies evaluating small and large floods together have shown how large floods can be preferentially generated by a subset of flood-generating mechanisms operating in a region and may thus have different seasonality than smaller floods (Collins et al., 2014; Hirschboeck, 1987; Smith et al., 2010, 2018; Tarasova et al., 2020; Villarini & Smith, 2010). It is therefore possible that large floods could show different trends and large-scale climate associations as well (Bertola et al., 2020; Villarini et al., 2014).

In this contribution, our aim is to characterize large floods across CONUS in the modern hydroclimate period. We focus on the period 1966–2015 because many studies have documented step changes in CONUS streamflow regimes, including floods, at approximately 1970 (Armstrong et al., 2014; Collins, 2009; McCabe & Wolock, 2002; Ryberg et al., 2020; Villarini & Smith, 2010). This 50 yr period thus reflects mostly contemporary conditions while also maximizing record length, the number of available gages, and regional coverage. Our first objective is to describe, in detail, the seasonality of the 10 largest and 2 largest floods in our data set. With that information, we address these questions: (a) Can large-flood seasonality be different from that of all AMS floods across CONUS regions? (b) How strong is the seasonality of large floods in each region? (c) Do some regions have multiple seasons for large floods? (d) Does large-flood seasonality change with increasing flood magnitude? Our second

objective is to determine whether large floods have become more or less frequent with time across CONUS for the period 1966–2015. To address this question, we complement a traditional type of Poisson regression for count-based trend analyses with a novel method based on expected occurrence. The third objective is to evaluate whether there are any relationships between the occurrence of large floods across CONUS and indices of climate variability.

2. Methods

2.1. Large-Flood Data

Large floods are defined in this study as the 10 largest AMS floods observed at a streamgage over the 50 yr period from water year 1966 through water year 2015 (with corresponding calendar year dates from October 1, 1965 through September 30, 2015; hereafter simply “1966–2015”). Over this record length, the 10 largest instantaneous flood peaks at a station have empirical recurrence intervals ranging from 5 yr (10th largest event) to 50 yr (largest event). For most analyses, we separately investigated the 2 largest AMS floods in the same period at each streamgage.

Streamgages across CONUS were identified from the U.S. Geological Survey's (USGS) Hydro-Climatic Data Network 2009 (HCDN-2009; Lins, 2012), which is a subset of USGS streamgages classified as minimally altered by upstream reservoir regulation, urbanization, or other direct human watershed alterations. From this network, the set of streamgages was further narrowed based on record completeness criteria used in Dudley et al. (2018) and Hodgkins et al. (2019), which require that each decade of annual flood peaks have at least 8 observations, or 80% completeness, to assure that there are no long periods of missing data. Annual, instantaneous flood peaks meeting these criteria resulted in 496 streamgages (Figure 1a).

A final restriction of the data set was to remove nested streamgages that could affect the power of the statistical tests because of high spatial cross-correlation. Falcone (2011) lists HCDN-2009 streamgages that are nested and the basins they are nested within. Of the 496 streamgages that met our criteria, 39 are nested. We wanted to maximize the number of sites available for analysis while also ensuring that nested streamgages with high cross-correlations of annual flood peaks were removed, so we did further analyses to retain as many of these 39 streamgages as possible. For pairs of nested sites, the percent nested (the percent to which one basin area overlaps with the basin area of the nested streamgage) was plotted versus the Pearson r cross-correlation between the natural logs of the annual flood peaks (Figure 1b). Streamgages with greater than 20% nestedness tend to have correlations in annual peak flows greater than 0.9 (Figure 1b), therefore these streamgages were removed from further analysis, reducing the total number of streamgages by 23 to a final set of 473 streamgages (Figure 1a). Basin sizes in our final set range from 2 to 12,850 km² (10th, 50th, and 90th percentiles are approximately 50, 360, and 1,780 km², respectively).

For each of the final 473 streamgages, AMS floods over the 50 yr period of record were then obtained from the National Water Information System (U.S. Geological Survey, 2020). The 10 largest and 2 largest floods were identified by ordering the AMS series and using only the floods of these ranks in the period. The streamgages, 10 largest floods with their rank, and corresponding dates can be found in Archfield et al. (2022).

Analyzing large floods exclusively presents sample size challenges for some analyses. For example, the seasonality of the 10 largest floods cannot be characterized meaningfully for one gage. Nor is it meaningful to pool data for all 473 CONUS streamgages to characterize large-flood seasonality given the heterogeneity of hydroclimatic conditions and flood-generating mechanisms across the country. Thus, for our seasonality investigations, we grouped streamgages into 14 geographically coherent gage clusters identified by McCabe and Wolock (2014) that correspond to climatic and physiographic regions across the country (Figure 1c). Data pooled this way were also used to analyze regional trends in annual and seasonal counts of large floods and relationships between large-flood occurrence and climate indices. We considered other regionalization approaches, like clustering based on the seasonality of all annual maximum floods, but doing so would complicate our investigation of whether the seasonality of large floods can be different from that of all floods. Clustering based on the McCabe and Wolock (2014) regions, which as noted are geographically coherent and correspond to CONUS climatic and physiographic regions, is appealing because hydroclimatology and physiography are important influences on the generating mechanisms for both large and small floods in a region.

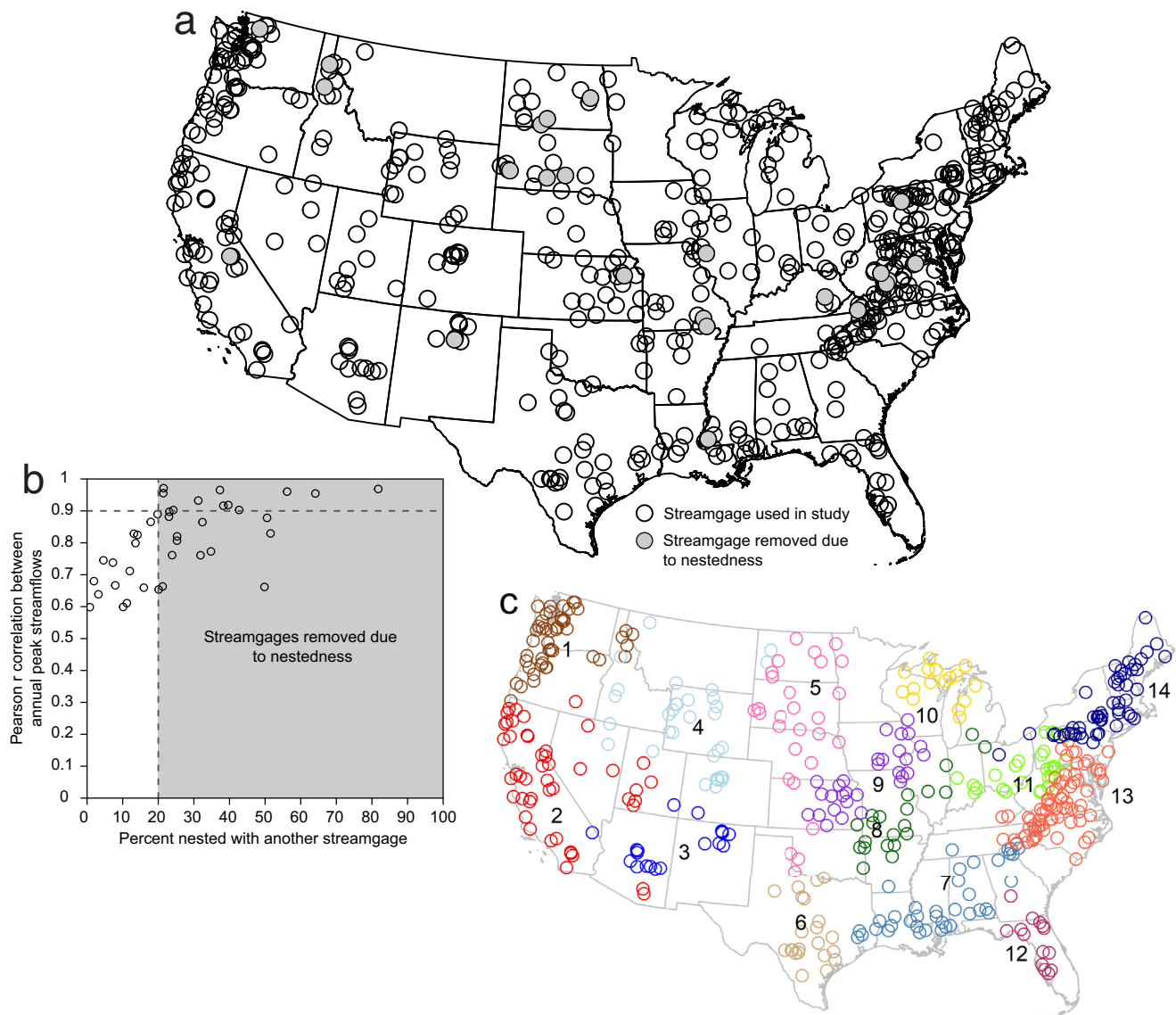


Figure 1. U.S. Geological Survey streamgages used to characterize large-flood occurrence across the conterminous United States (CONUS) during the study period (1966–2015) and those not used because their basin areas have greater than 20% overlap with another streamgage (a). Plot of the percent to which basin area overlaps with another streamgage, represented as percent nested, and the Pearson r cross-correlation between the natural logs of the annual peak flow series (b). Fourteen regions with similar hydroclimatic and physiographic conditions that were used to characterize large-flood seasonality across CONUS and investigate regional trends (c). The regions were first identified by McCabe and Wolock (2014).

For 87 of our 473 gages that were not already grouped by McCabe and Wolock (2014), we assigned them to a region via their clustering procedure. This required us to compute the annual means of the daily flows from 1951 to 2009 (their study period) for each cluster, standardize them by the mean and variance, and compute the annual means of the daily flows for each unclassified gage for the same period. We then computed the Pearson r correlation between the annual mean for each unclassified gage and each annual cluster mean, assigning gages to the cluster with the highest correlation. All but 5 gages had a cluster with a correlation >0.5 and all but 2 had a cluster with a correlation >0.3 .

2.2. Climate Indices

Relationships between large-flood occurrence and indices of climate variability were examined for the Atlantic Multidecadal Oscillation (AMO), NAO, Pacific Decadal Oscillation (PDO), Pacific North American pattern (PNA), and ENSO. The AMO is an index of North Atlantic sea-surface temperatures with a 65–80 yr periodicity (Enfield et al., 2001). The NAO (Hurrell et al., 2003) represents the atmospheric pressure gradient in the North Atlantic Ocean between a station in the Azores and a station in Iceland; it has quasi-periodic biennial and 6–10 yr oscillations (Hurrell & Van Loon, 1997). The PDO (Mantua & Hare, 2002), the leading principal component of sea-surface temperature anomalies in the North Pacific Ocean, has a 10–25 yr periodicity. The PNA (Wallace & Gutzler, 1981) reflects a quadrupole pattern of 500 mbar height anomalies, with anomalies of similar sign located south of the Alaskan Aleutian Islands and in the southeastern United States; opposite-signed anomalies are located near Hawaii, and the Canadian Rocky Mountains during the winter and fall (NOAA, 2020c). It has a quasi-periodic variation of 3–4 yr (Leathers & Palecki, 1992). ENSO reflects the interaction of large-scale warming or cooling of the central eastern equatorial Pacific Ocean and the Southern Oscillation, a large-scale atmospheric pressure pattern across the tropical Pacific, with a periodicity of 2–7 yr (Tootle et al., 2005).

Monthly values were downloaded for the unsmoothed AMO (NOAA, 2019), NAO (NOAA, 2020a), PDO (NOAA, 2020b), PNA (NOAA, 2020c), and bivariate ENSO time series (NOAA, 2020d). Winter values of NAO (December–March) were averaged and lagged by one year for 1966–2015. Water-year averages were computed for 1966–2015 for the other four indices. NAO analyses focused on the lagged winter index (December–March) because the NAO is most strongly expressed at this time of year (Hurrell et al., 2003) and earlier analyses exploring NAO–river flood relationships in two CONUS regions found the strongest associations with the winter index lagged by one year (which is a 6 months lag with the water year; Armstrong et al., 2014; Collins, 2009).

2.3. Large-Flood Seasonality

We identified flood seasons at a monthly resolution using a probabilistic method proposed by Cunderlik et al. (2004). We pooled the 10 largest floods from the streamgages in each of our 14 regions, grouped them by month, and then adjusted the monthly relative frequencies to reflect 30-day months for all months using the method of Mardia (1972). The observed monthly frequencies (i.e., probabilities) were then compared with the expected variability of non-seasonal monthly frequency distributions to determine if a given month was significantly flood-rich or flood-poor. To do so, one-sided 95% confidence intervals were computed from models given by Cunderlik et al. (2004) that were based on empirical distributions of monthly frequencies generated from a non-seasonal model—the circular uniform distribution—via a large number of Monte Carlo simulations (100,000). There are equal chances of a flood happening in any month in a synthetic flood record developed from the circular uniform distribution (1 in 12, or 8.33%). The confidence bounds generated by this method are narrower for simulations with a greater number of observations. Thus, in our application, regions with more stations have narrower confidence intervals. The Cunderlik et al. (2004) confidence interval models are applicable from 30 to 500 observations. Regions 13 and 14 exceed the upper bound (710 and 540 observations for the 10 largest floods, respectively), but we found that confidence intervals computed assuming 500 observations for these regions did not significantly change the results.

To address sampling variability in the observations, each regional record was also resampled 1,000 times (Cunderlik et al., 2004). The confidence intervals and resampling results were then applied as follows to determine the probability of a given month being significantly flood-rich or flood-poor. Observed monthly frequencies that exceeded the upper confidence bounds, and also had greater than 10% of resamples exceeding those bounds, are statistically significant flood-rich months—like November, December, January, and February in Region 1 shown in dark blue (Figure 2a). Similarly, monthly frequencies that did not exceed the lower bounds (and with greater than 10% of resamples also failing to exceed those bounds) are significant flood-poor months (shown in dark brown). Monthly frequencies were considered “possibly significant” flood-rich or flood-poor if they were within the confidence bounds, but greater than 10% of resamples were outside the upper or lower bound, respectively. All other months were identified as not significant.

The seasonality of the 2 largest floods in each region was identified by simply computing monthly relative frequencies because there were not enough data to justify the probabilistic method. As with the 10 largest floods,

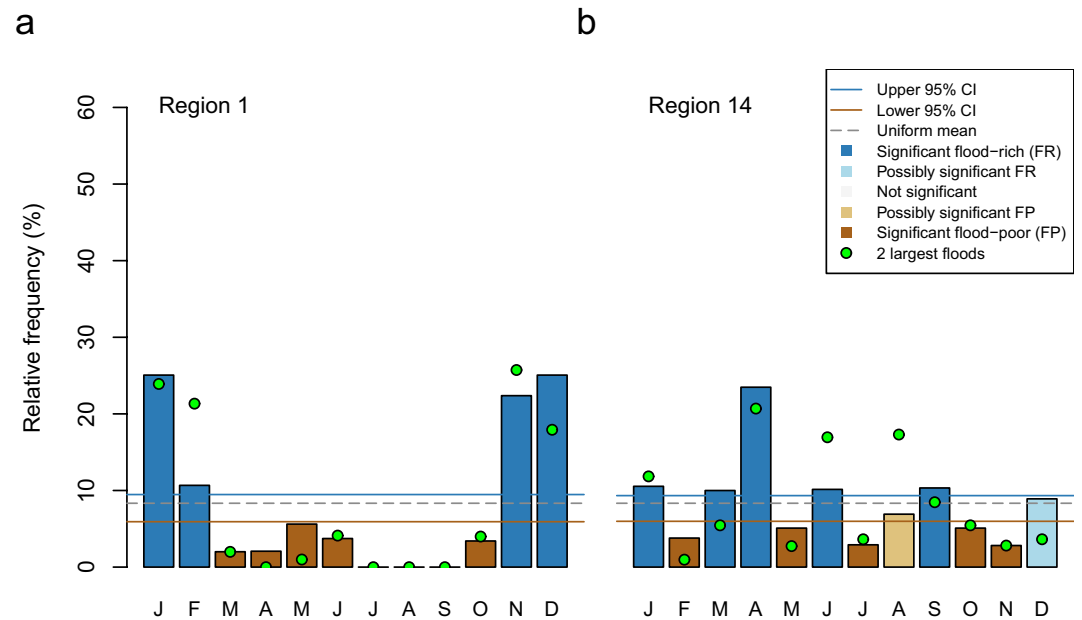


Figure 2. Large-flood seasonality for Regions 1 and 14 in the conterminous United States for water years 1966–2015. Colored bars are the monthly frequencies of the 10 largest floods pooled for all stations in each region. Monthly frequencies for pooled 2 largest floods are indicated with green dots. Water year is the 12-month period beginning October 1 of the previous calendar year and ending September 30 of the current calendar year. CI, confidence interval.

these were adjusted so that all months have 30 days (Mardia, 1972). The monthly frequencies of the 2 largest floods are shown as green dots in Figure 2, superimposed on the monthly frequencies of the 10 largest floods.

To investigate whether the seasonality of large floods can be different from the seasonality of all AMS floods in our regions, we computed monthly relative frequencies for each region by pooling the full 50 yr AMS records for each site. These too were adjusted by the Mardia (1972) method so that all months have 30 days. As with the 2 largest floods, we did not employ the probabilistic method for the full 50 yr AMS distributions because statistical significance depends strongly on sample size. Sample sizes differ by a factor of 5 in each region between the 10 largest floods and the full 50 yr AMS, so comparing the significance of a given month or months between the large-flood distributions and the full AMS distributions is not meaningful. We investigated other methods to quantitatively compare the large-flood and full AMS monthly frequency distributions for each region, but most require independent samples. The distributions for the 10 largest and 2 largest floods are subsets of the full AMS distributions and thus are not independent. We, therefore, focused on qualitatively comparing the shapes of the full AMS distributions with those of the large floods (10 and 2 largest taken together) in each region.

2.4. Expected and Observed Probabilities of Large-Flood Occurrence

Here, we introduce a novel and generalizable method based on expected occurrence for evaluating whether the frequency of large floods across CONUS has changed in the modern hydroclimate. We compared the actual observed numbers of 10 largest and 2 largest floods that occur in the latter half of the study period (most recent 25 yr; 1991–2015) with the numbers of largest floods expected to be observed over that period. We then repeated this experiment to compare the actual versus expected numbers of 10 largest and 2 largest floods for the last 10 yr of the study period (2006–2015). The methods of computing these probabilities can be applied to any period within the full record. However, for the purposes of this study, we are looking only at the later periods to determine if large-flood occurrence is more prevalent in recent years.

For each of the 473 CONUS streamgages, the number of 10 largest and 2 largest floods for the study period (1966–2015) that occurred in the last 25 yr (1991–2015) and last 10 yr (2006–2015) were counted. For the evaluations of the 10 largest floods, each streamgage was placed in one of 11 bins, labeled zero to 10, corresponding to the number of times the 10 largest floods occurred during the recent 25 or 10 yr period of interest, respectively,

for that streamgage. For the 2 largest floods, each streamgage was put into one of three bins, labeled zero to two, corresponding to the number of times the 2 largest floods occurred during the recent 25 or 10 yr period of interest, respectively, for that streamgage.

To compute the expected number of times the M -largest floods (in this case the 10-largest and 2-largest) would occur over an N -year period of interest, two independent approaches—one using a simulation experiment and one using combinatorics principals from probability theory—were applied to cross-verify results.

The simulation experiment was designed as follows. For each of the 473 streamgages, we obtained the water years with available data (recall that only 8 of every 10 yr in each decade were required to have a flood peak value). From those water years, M years were randomly chosen and assigned exactly one random number from $1 \dots M$ without replacement. This created a simulated data set of M -largest floods where the year of occurrence and rank of each large flood was randomly assigned, as would be expected if the frequency of occurrence of large floods were random and not changing with time. This random assignment of M ranks to M years for the 473 streamgages was repeated 1,000 times and the counts of streamgages were averaged for each of the 0, 1, ..., M bins to obtain the expected numbers of the M -largest floods occurring over the M -year period of interest. The 90% confidence intervals were also extracted from the simulation experiment results by computing the 0.05 and 0.95 quantiles from the 1,000 simulation runs for each bin.

To compute the expected frequencies using combinatorics principals from probability theory, the solution can be formulated by first enumerating all arrangements that the M -largest floods can be ordered across the 50 yr study period (1966–2015). This number of arrangements is a permutation, solved by $P(n, r) = n!/(n - r)!$, where $P(n, r)$ is the number of different arrangements of r elements selected from n objects—in this case the number of different ways to arrange the M -largest floods (r) across 50 yr of record (n). Thus, we have $P(50, M) = 50!/(50 - M)!$. When the set of all possible arrangements is enumerated, this results in all possible subsets of years in which the M -largest floods could have occurred if the floods were expected to occur randomly throughout the full period of record. Enumeration was executed using the `approxPerm` function in the `gtools` library (Warnes et al., 2020) built for `R` (R Core Team, 2019). Each enumerated arrangement is evaluated to determine whether 0, 1, ..., or M of the M -largest floods occurred over the N -year period (e.g., the last 25 and last 10 yr of the study period) and placed in the appropriate 0, 1, ..., or M bin. After all arrangements have been placed in the appropriate bins, the values in each bin are summed and divided by $P(50, M)$ to obtain the expected probabilities of 0, 1, ..., or M of the M -largest floods occurring over the N -year period of interest. Lastly, we multiply each of these probabilities by 473 to obtain the number of streamgages expected to appear in each of the occurrence bins.

2.5. Trends and Relations With Climate Indices

The annual occurrence of the 2 largest and 10 largest floods at individual streamgages were aggregated for the entire CONUS and for the 14 study regions. The number of large floods in each water year from 1966 to 2015 were summed for all streamgages in CONUS and for all gages in each region. These national and regional time series were used to investigate temporal trends in large-flood occurrence and for interannual relations between the annual number of large floods and climate indices.

Temporal trends in large-flood occurrence, and interannual relations between occurrence and climate indices, were also analyzed seasonally. For each region, the number of 2 largest and 10 largest floods in each flood-rich season were summed to create seasonal time series from 1966 to 2015. Flood-rich seasons in a region were either single or contiguous flood-rich months as defined in Section 2.3. For example, Region 1 has one flood-rich season for large floods: November–February (Figure 2a). Region 14 has four flood-rich seasons: January, March–April, June, and September (Figure 2b). To avoid individual years having undue influence on the analyses, seasonal time series for a region were required to have at least 10 yr with a non-zero number of large floods. This resulted in the censoring of results from sixteen 2 largest (Tables S2 and S4 in Supporting Information S1) and three 10 largest seasonal time series, out of 25 total seasonal series (Tables S3 and S5 in Supporting Information S1).

We computed temporal trends in large-flood occurrence and relations between interannual flood occurrence and the five climate indices using a modification of Poisson regression. Poisson regression is a type of generalized linear model appropriate for count data (McCullagh & Nelder, 1989). The annual number of flood occurrences is often assumed to follow a Poisson distribution (Mediero et al., 2015). A Poisson distribution assumes that the number of occurrences in different years is identically and independently distributed, however, the presence of

clusters of flood-rich and flood-poor years violates this assumption (Lun et al., 2020; Mediero et al., 2015; Villarini et al., 2011). The degree of departure from a Poisson process can be characterized by a dispersion index; overdispersion can be caused by clustering or other unexplained variability that leads to larger variability in the annual number of occurrences than is expected for a Poisson process (Mediero et al., 2015; Villarini et al., 2011). A dispersion index can be computed by dividing the chi-square statistic of a Poisson model (reflecting the deviation of the predicted from the observed values) by the degrees of freedom (Frome & Checkoway, 1985; Nussbaum et al., 2008). If the dispersion index is much greater than 1.0, this is a sign of overdispersion (Nussbaum et al., 2008); the index can be used to account for the degree of departure from a Poisson process.

The national and regional time series of 2 largest and 10 largest floods in this study showed overdispersion. The dispersion index was calculated as the sum of the squared Pearson's residuals divided by the degrees of freedom. For the 2 largest and 10 largest flood occurrence for 1966–2015, the dispersion index for the national group was 10.4 and 12.0, respectively. For the 14 regional groups, the median dispersion index was 2.7 and 3.3, for the 2 largest and 10 largest time series, respectively; the minimum index was 1.4 and 2.4 while the maximum index was 7.3 and 9.5.

Because of overdispersion, we computed the magnitude and significance of temporal trends in annual and seasonal large-flood counts over the study period with quasi-Poisson regression in *R* (R Core Team, 2019) using a generalized linear model, `glm` (formula = Counts ~ Years, family = quasi-Poisson [link = "log"]), which accounts for overdispersion. We also used quasi-Poisson regression to investigate the magnitude and significance of relationships between annual and seasonal time series of large-flood counts and five climate indices (AMO, NAO, PDO, PNA, and ENSO) by replacing Years with the appropriate climate index for each year. Separately, to determine the amount of explained interannual variance in the relations between large-flood counts and climate indices, we computed Pearson's *r* via the `cor.test` function in *R*, squared them, and reported them in percent (R Core Team, 2019).

3. Results

3.1. Large-Flood Seasonality

The 10 largest floods exhibit pronounced seasonality, reflected in strongly unimodal monthly frequency distributions, in the Far West (Regions 1, 2), the Intermountain West (4), and across the Plains and parts of the Upper Midwest (5, 9, 10; Figure 3). Large-flood seasonality is weaker (i.e., no month $\geq 20\%$ relative frequency) or more complex (i.e., multimodal) in the Southwest and Texas (3, 6), Gulf Coast (7, 12), Lower Mississippi and Ohio Valleys (8, 11), and the eastern United States (13, 14). In these latter areas, there can be multiple, distinct seasons for large floods (e.g., Regions 12 and 14) or occurrence can be diffuse with large floods occurring several months throughout the year (e.g., Region 11). The monthly frequencies of the 2 largest floods generally follow the relative magnitudes of the monthly frequencies for the 10 largest floods in a given region (e.g., Figure 2a), but regions with weak and/or complex seasonality more frequently show departures (e.g., Figure 2b). Detailed monthly frequency plots for each region are shown in Figure S1 in Supporting Information S1.

When we compare the seasonality of large floods (both 10 and 2 largest) to all AMS floods, we find that some regions generally have similarly shaped monthly relative frequency distributions—e.g., the Intermountain West (Region 4), Gulf Coast (7), and Upper Midwest (10; Figures S1 and S2 in Supporting Information S1). Others show only moderate, yet potentially important, differences. For example, in the Northwest (Region 1), most AMS floods occur from November–May, especially November–December–January, but large floods are more concentrated in November–February while March–May is considerably less important. In some regions, the differences are more pronounced, for example, the Ohio River Basin (Region 11), Mid-Atlantic (13), and Northeast (14). In these areas, the winter and early spring months are most important for all AMS floods and the warm season is generally flood-poor, but for large floods—especially the 2 largest—the warm season has greater relative importance.

3.2. Expected and Observed Probabilities of Large-Flood Occurrence

The occurrence of the 10 largest floods in the latter half of the study period (1991–2015) was not different from what was expected over the same period (Figure 4a), with the observed number of streamgages matching nearly

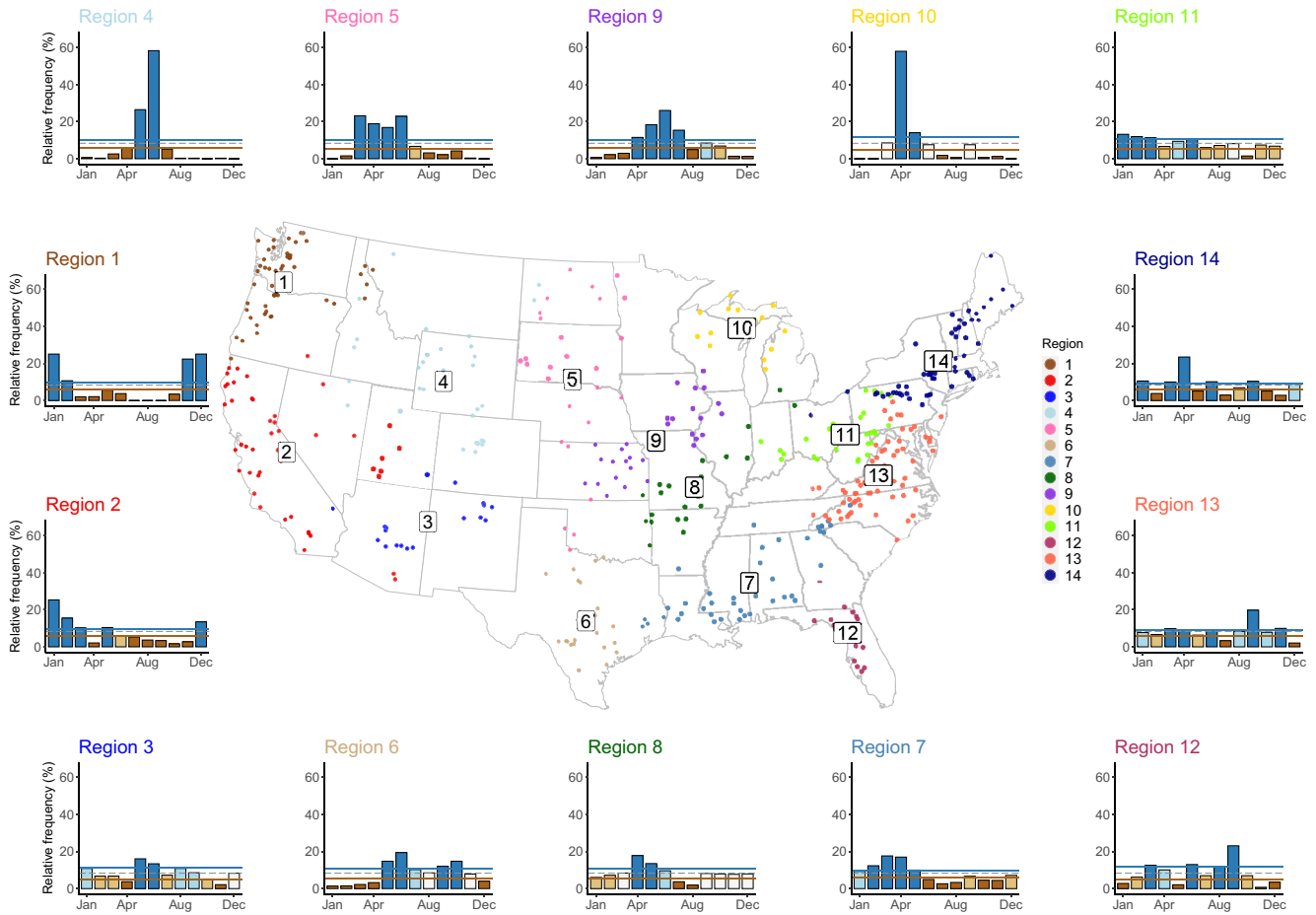


Figure 3. Monthly frequency distributions for large floods (10 largest) in the 14 regions identified by McCabe and Wolock (2014) with similar hydroclimatic and physiographic conditions, water years 1966–2015. Water year is the 12-month period beginning October 1 of the previous calendar year and ending September 30 of the current calendar year. See Figure 2 for detailed bar chart key.

exactly the expected number of streamgages for each bin of 10 largest flood counts. For bins where the expected number of streamgages did not match the observed (4, 6, 7, and 8; Figure 4a), the values were still within the confidence intervals.

Although the occurrence of the 10 largest floods in the latter half of the study period is consistent with what is expected by chance across CONUS, it is worthwhile to evaluate if there is any spatial cohesion to the streamgages that fall into the bins with the smallest and largest counts of the 10 largest floods. For example, if one region of CONUS contained all of the streamgages for which 8 of the 10 largest floods occurred in the latter half of the study period, this could indicate important changes in regional flood-generating mechanisms. To make this assessment, bins that contained less than 15% of the streamgages (the highest and lowest numbers of large floods; Figure 4a) were mapped (Figures 4b and 4c).

For streamgages where 3 or less of the 10 largest floods have occurred in the last half of the study period, few spatial patterns emerge with the exception of streamgages located in the Southeast extending from Louisiana to Virginia and parts of the Southwest and Intermountain West (Figure 4b). For streamgages where 7 or more of the 10 largest floods occurred in the last half of the study period, some spatial cohesion is apparent in the Pacific Northwest, the eastern edge of the Rocky Mountains, parts of the Plains and Midwest, the Texas portion of the Gulf Coast, and the Mid-Atlantic (Figure 4c).

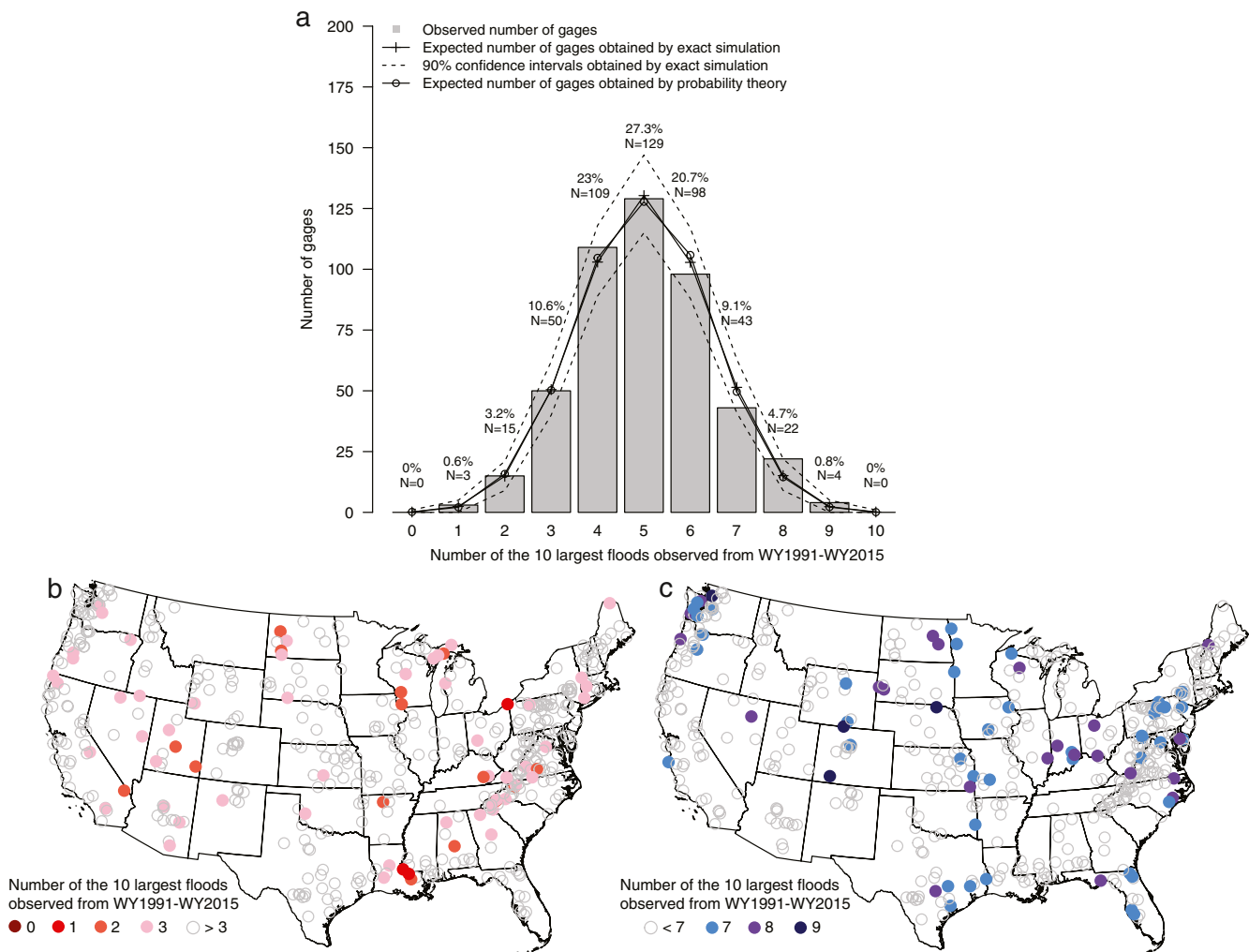


Figure 4. Comparison of the number of the 10 largest floods observed in the latter half of the study period (1991–2015) to the expected number over the same period. Values above the bars indicate percentages and counts of streamgages in a given bin (a). Maps showing the locations of the number of the 10 largest observed floods for bins that contain less than 15% of the streamgages (b and c). WY, water year: the 12-month period beginning October 1 of the previous calendar year and ending September 30 of the current calendar year.

When examining the frequency of occurrence of the 10 largest floods over the last 10 yr of the study (2006–2015), there is also little difference between the observed and expected number of streamgages for each bin (Figure 5a). However, there are a few observed values that fall nearly outside of the 90% confidence intervals: (a) the number of times zero of the 10 largest floods were observed in the last 10 yr was greater than expected, (b) the number of times 3 of the 10 largest floods were observed in the last 10 yr was less than expected, and (c) the number of times 4 of the 10 largest floods were observed in the last 10 yr was less than expected (Figure 5a). This would indicate that, if the largest floods were randomly distributed throughout the study period, there would be an expectation to see more large floods than were observed in the last 10 yr of the study period.

Mapping those bins containing less than 15% of the streamgages (Figure 5a) results in similar spatial patterns to those mapped in Figure 4b for bin values where 3 or less of the 10 largest floods have occurred in the last half of the study period. That is, the Southeast United States has clear spatial cohesion for streamgages where zero of the 10 largest floods were observed in the last 10 yr (Figure 5b). Spatial patterns for the streamgages where 4, 5, or 6 of the 10 largest floods were observed in the last 10 yr of the record are less obvious, although the Northeast, Midwest, and Pacific Northwest show some clustering (Figure 5b).

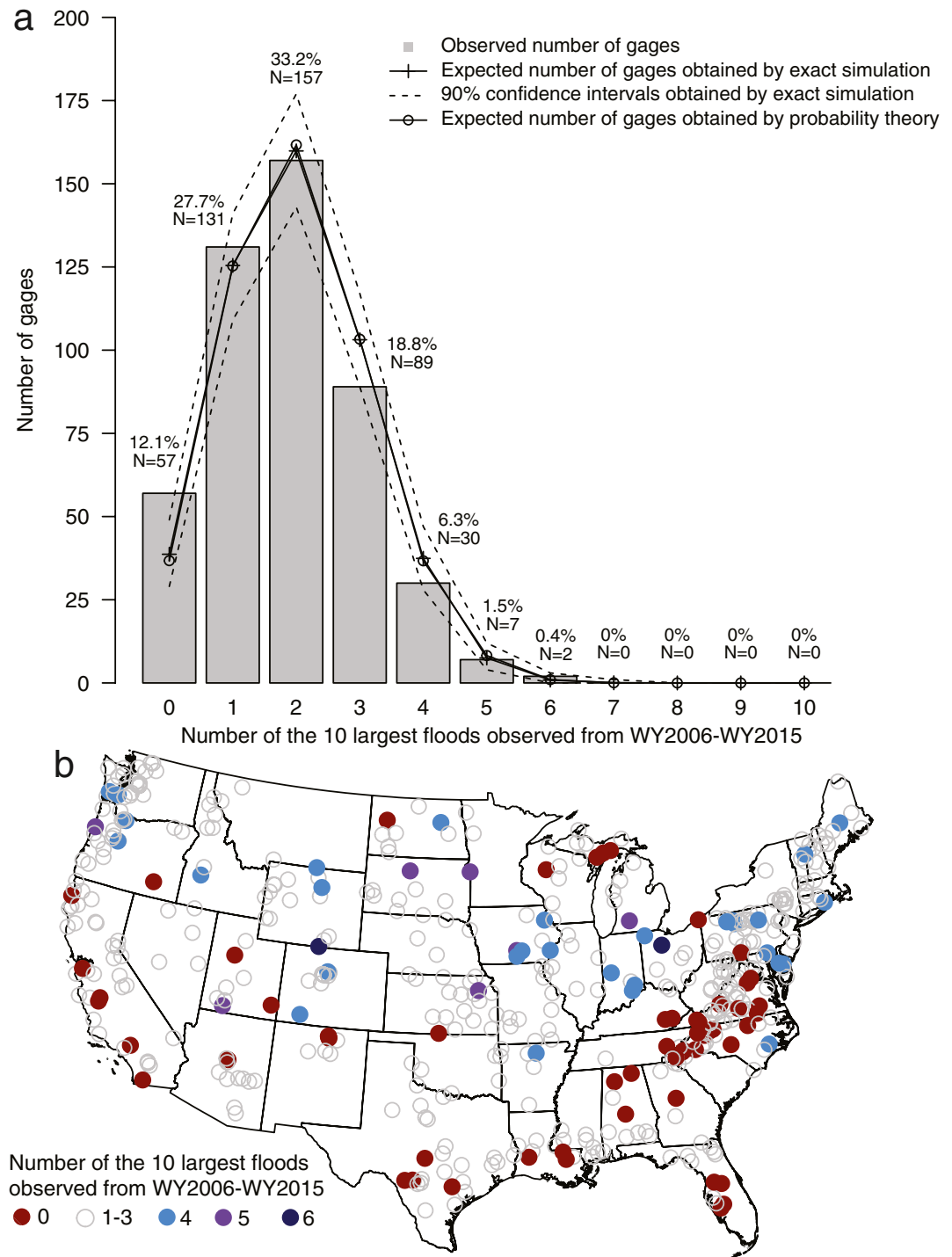


Figure 5. Comparison of the number of the 10 largest floods observed in the last 10 yr of the study period (2006–2015) to the expected number over the same period. Values above the bars indicate percentages and counts of streamgages in a given bin (a). Map showing the locations of the number of the 10 largest observed floods for bins that contain less than 15% of the streamgages (b). WY, water year: the 12-month period beginning October 1 of the previous calendar year and ending September 30 of the current calendar year.

The occurrence of the 2 largest floods over the last half and the last 10 yr of the study period were within the expected 90% confidence intervals (Figures 6a and 6b, respectively). The only bin that contained less than 15% of the streamgages was the bin with gages that had 2 occurrences of the 2 largest floods over the last 10 yr

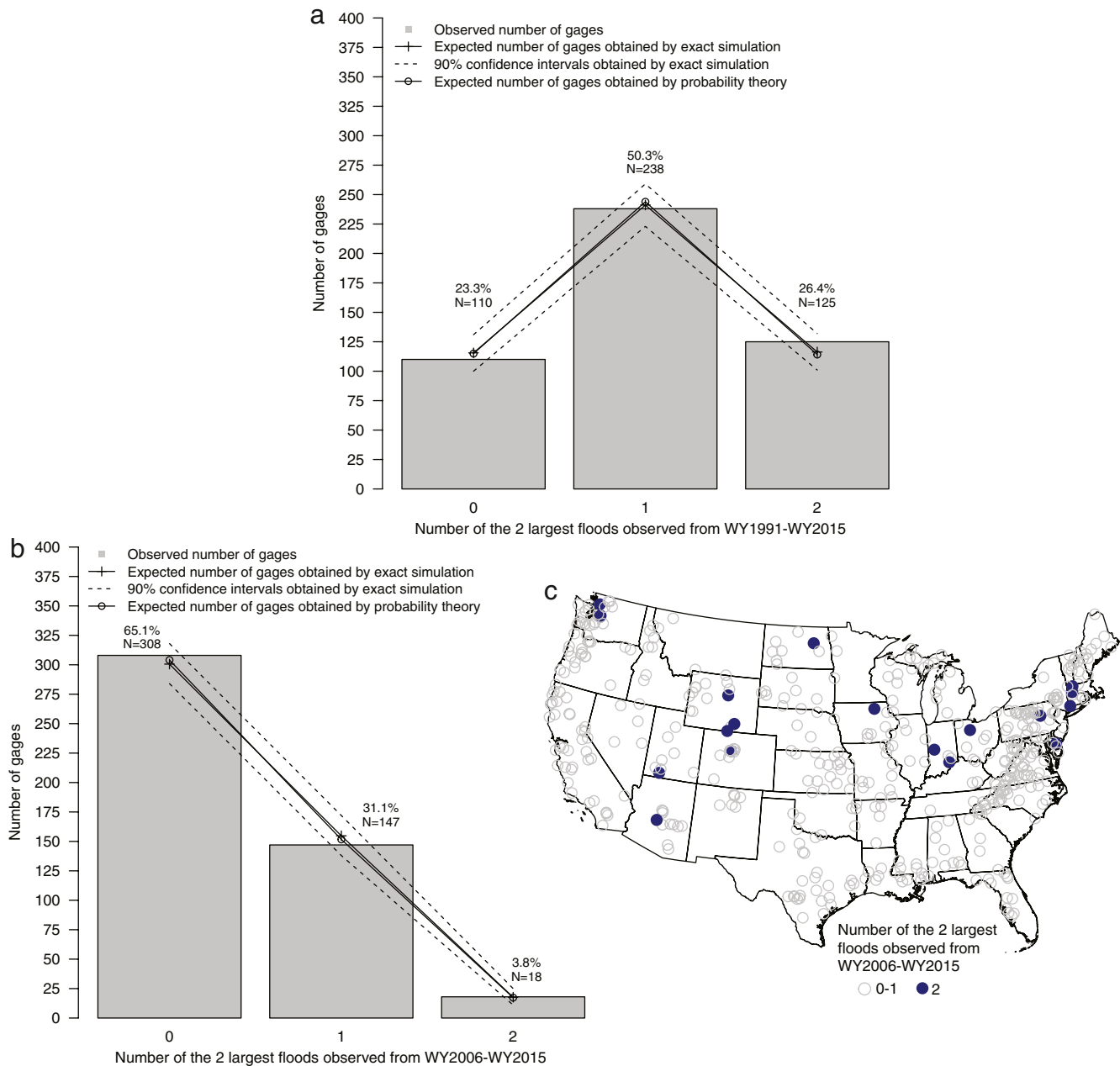


Figure 6. Comparison of the number of the 2 largest floods observed in the last half of the study period (1991–2015) (a) and the last 10 yr of the study period (2006–2015) (b) to the expected numbers over the same periods, respectively. Values above the bars indicate percentages and counts of streamgages in a given bin. Map showing the locations of the number of the 2 largest observed floods for bins that contain less than 15% of the streamgages (c). WY, water year: the 12-month period beginning October 1 of the previous calendar year and ending September 30 of the current calendar year.

(Figure 6b). Some clustering of those streamgages is evident in parts of the West, Midwest, and Northeast, but these patterns are weak (Figure 6c).

We examined the sensitivity of these analyses to the choice of analysis window (e.g., 15 yr rather than 25 or 10) and the period analyzed (e.g., the first 25 and 10 yr of record rather than the last 25 and 10 yr) and find that our general result—that large-flood occurrence across CONUS has not changed in the recent past—is not sensitive to these choices (Figure S3 in Supporting Information S1; Lun et al., 2020).

While there were no clear increases or decreases in the occurrence of large floods in the most recent 25 and 10 yr of the study period across CONUS, our analyses did reveal 22 streamgages that have a predominance of the

Table 1
Trends in Annual Counts of Large Floods Over the Period 1966–2015 for All of the Conterminous United States (CONUS) and the 14 Regions

	CONUS	Regions													
		1	2	3	4	5	6	7	8	9	10	11	12	13	14
2 Largest															
<i>p</i> -value	0.93	0.41	0.39	0.55	0.20	0.27	0.58	0.09	0.63	0.66	0.54	0.44	0.79	0.33	0.33
Trend	−0.64	1.54	−1.16	−0.35	1.32	−0.77	−0.34	−1.87	0.34	0.34	−0.36	0.65	0.11	−2.01	1.90
10 Largest															
<i>p</i> -value	0.79	0.61	0.19	0.23	0.62	0.95	0.70	0.07	0.31	0.70	0.27	0.08	0.71	0.76	0.49
Trend	−4.41	2.14	−5.73	−2.20	1.54	0.13	−0.67	−5.56	1.65	0.78	−1.55	3.06	0.49	−1.68	3.14

Note. Bold *p*-values are significant at $p < 0.1$. The trend magnitudes represent the difference in the number of floods per year over the 50 yr period, as computed by quasi-Poisson regression.

10 largest floods in both the most recent half and the most recent 10 yr. Six of the 22 streamgages also recorded both of their 2 largest floods in the most recent 10 yr. Because the focus of our investigation is at the regional and continental scale, and these gages with unusual temporal occurrence patterns do not show any particular spatial clustering, further analyses are outside the scope of this study. However, we compiled information about these outlier streamgages in the supplement to support future local studies (Text S1 and Table S1 in Supporting Information S1).

3.3. Regional and National Trends

There was an insignificant decrease ($p \geq 0.1$) in the number of the 2 largest annual floods across CONUS from 1966 to 2015 (all stations in CONUS grouped), a significant decrease ($p < 0.1$) for Region 7 (Gulf Coast), and a mix of insignificant increases and decreases for the remaining 13 regions (Table 1, Figure 7). For the 10 largest annual floods, there was an insignificant decrease for CONUS, a significant decrease for Region 7 (Gulf Coast) and a significant increase for Region 11 (Ohio River Basin; Table 1, Figure 8). For Region 7, the average annual count of the 2 largest and 10 largest floods decreased by 1.9 and 5.6 floods per year, respectively, from 1966 to 2015; for Region 11 the average annual count of the 10 largest floods increased by 3.1 over the same period. When large floods were parsed into seasons for the regions, there were significant decreases ($p < 0.1$) in the number of the 2 largest and 10 largest floods from 1966 to 2015 for Region 7 (Gulf Coast) in February–May (Tables S2 and S3 in Supporting Information S1).

3.4. Relations With Climate Indices

There was a significant negative relation ($p < 0.1$) between the number of the 2 largest floods across CONUS in each water year and the PNA pattern (Table 2), though the amount of explained interannual variance is very low (5.9%, Pearson's r^2). A negative relation with the PNA was also significant ($p = 0.002$) for the 2 largest floods in Region 10 (Upper Midwest) with explained variance of 17.4% and significant for Regions 5 (northern Great Plains), 11 (Ohio River Basin), and 13 (Mid-Atlantic). There were significant negative relations between the 2 largest floods and the AMO in Region 7 (Gulf Coast) and Region 10 (Upper Midwest). For the NAO, significant relations were found for four regions: positive relations with the number of the 2 largest floods in Regions 7 (Gulf Coast) and 9 (Midwest) and negative relations in Regions 4 (northern Rockies) and 5 (northern Great Plains). There were no significant relations between the annual number of the 2 largest floods and the PDO for any region. There were significant negative relations between the 2 largest floods and ENSO for Regions 4 (northern Rockies) and 14 (Northeast) and a significant positive relation with Region 6 (Texas).

As with the 2 largest floods, there was a significant negative relation ($p < 0.001$) between the annual number of the 10 largest floods and the PNA for Region 10 (Upper Midwest), with explained variance of 22.9%. There was also a significant negative relation ($p < 0.1$) with AMO (Table 2) which had explained variance of 9.3%. ENSO had significant positive relations between the numbers of 10 largest floods for four regions from California to Florida: Region 2 (mostly California), Region 3 (Southwest), Region 6 (Texas), and Region 12 (mostly Florida).

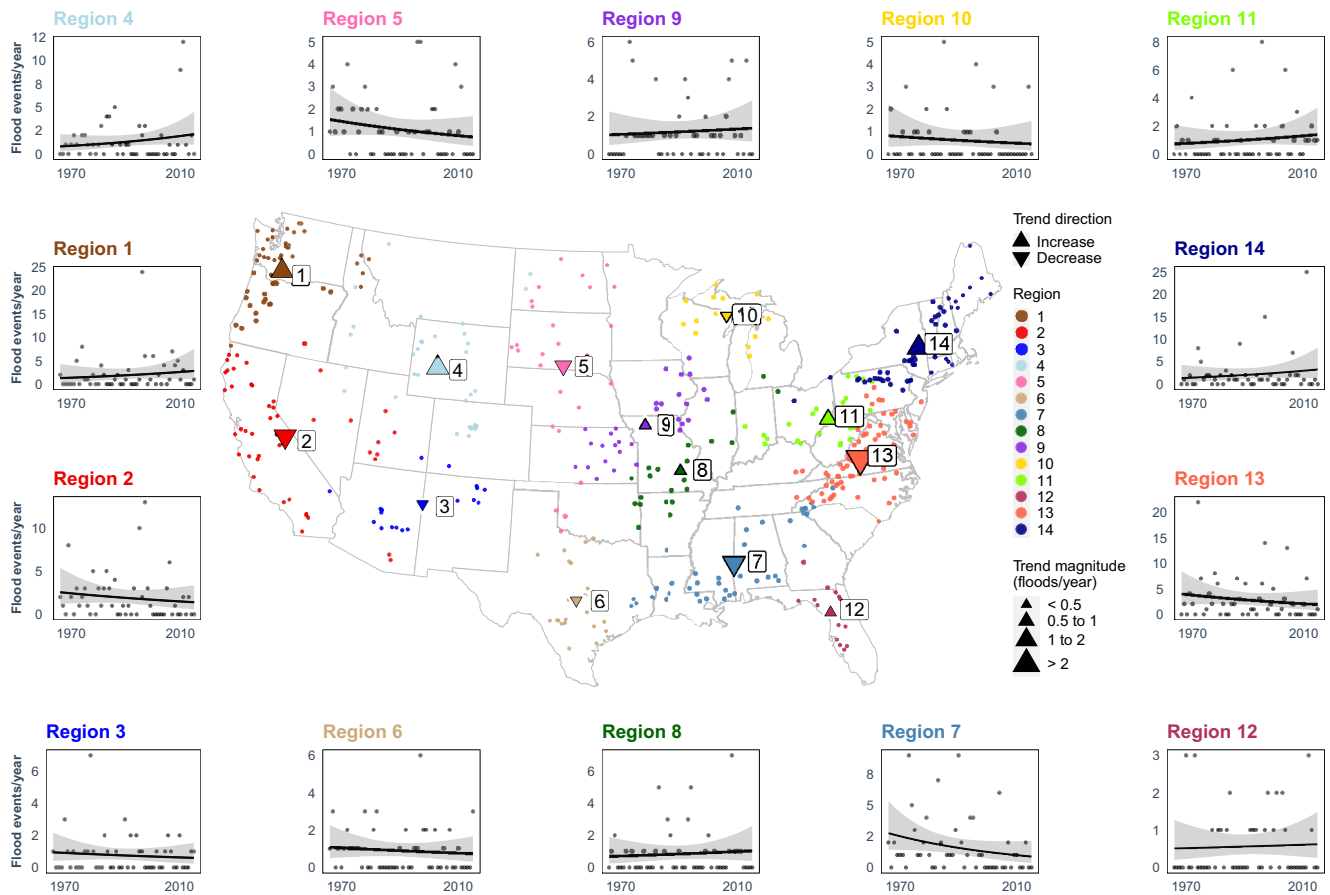


Figure 7. Trends in the 2 largest floods (flood events/year) for the study period for each of the 14 regions. Shaded areas are 95% confidence intervals.

Explained variance for these regions ranged from 6.1% to 13.7%. There was a significant positive relation with PDO for Region 2 and a significant positive relation with NAO for Region 9 (Midwest).

When large floods were parsed into seasons for the regions, significant relations between the 2 largest floods and climate indices were scattered across the regions and seasons (Table S4 in Supporting Information S1). There was a significant negative relation ($p < 0.1$) with PNA in Region 6 for September–October (Texas). A significant negative relation was found between the 2 largest floods and NAO in Region 5 (northern Great Plains) for March–June and a significant positive relation in Region 9 (Midwest) for April–July. There was a significant positive relation with PDO in Region 14 (Northeast) for March–April. A significant positive relation was seen for ENSO in Region 2 for December–March and Region 14 for March–April. There was a significant negative relation with AMO in Region 7 (Gulf Coast) for February–May.

Significant relations between the number of 10 largest floods and climate indices were found for several regions in selected seasons (Table S5 in Supporting Information S1). There were significant negative relations with PNA in Region 13 (Mid-Atlantic) for June ($p < 0.001$) and Region 10 (Upper Midwest) for April–May ($p = 0.002$). A significant negative relation ($p < 0.1$) with PNA was found in Regions 8 (Lower Mississippi Valley) for April–May and 14 (Northeast) for June along with a significant positive relation in Region 14 for March–April. There was a significant positive relation between the 10 largest floods and ENSO in Region 6 (Texas) for May–June ($p < 0.001$), along with significant positive relations ($p < 0.1$) in Region 2 (mostly California) for December–March, Region 3 (Southwest) for May–June, Region 13 (Mid-Atlantic) for March–April, and Region 14 (Northeast) for March–April. There was a significant positive relation ($p = 0.002$) with PDO in Region 6 for May–June and a significant positive relation in Region 2 for December–March, Region 13 for March–April, and in Region 14 for March–April. NAO had a significant positive relation in Region 9 (Midwest) for April–July. AMO had

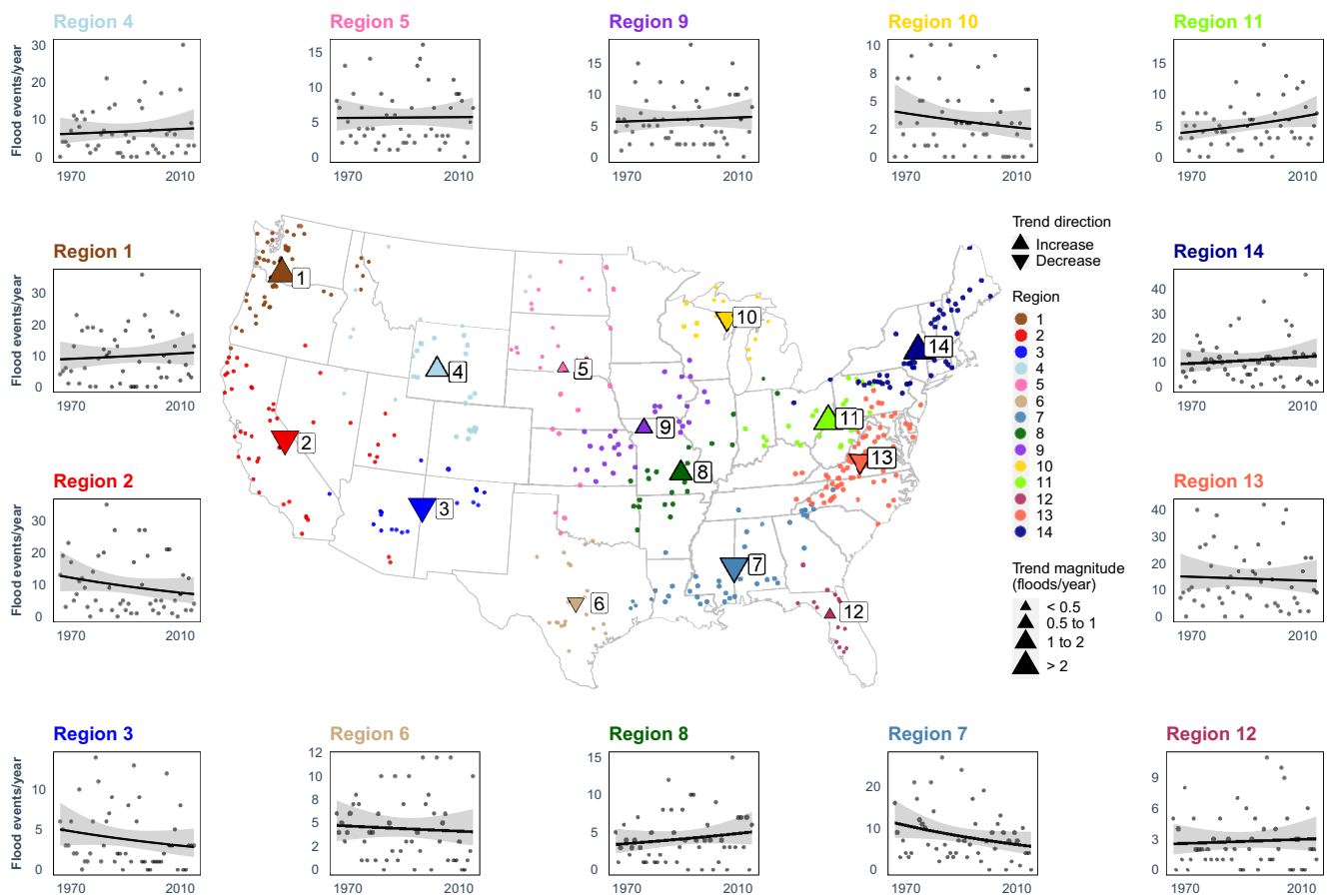


Figure 8. Trends in the 10 largest floods (flood events/year) for the study period for each of the 14 regions. Shaded areas are 95% confidence intervals.

significant negative relations with the 10 largest floods in Region 7 (Gulf Coast) for February–May and Region 13 (Mid-Atlantic) for June.

4. Discussion

4.1. Large-Flood Seasonality

Characterizing large-flood seasonality in detail is a useful first step for identifying the generating mechanisms for large floods in a region (Berghuijs et al., 2016; Collins, 2019; Collins et al., 2014; Hirschboeck, 1991; Ye et al., 2017). It also has practical utility for infrastructure operations and maintenance, forecasting, and preparedness. Strong large-flood seasonality, like we documented in Regions 1, 2, 4, 5, 9, and 10 (Figure 3), suggests that a relatively small number of mechanisms dominate large flood generation in these regions (e.g., Barth et al., 2017; Neiman et al., 2011). Where large-flood seasonality is weaker or more complex, as in Regions 3, 6, 7, 8, 11, 12, 13, and 14 (Figure 3), large floods may have a greater range of generating mechanisms. Large floods (10 and 2 largest) frequently have differences in seasonality than all floods in these regions (e.g., Regions 3, 11, 13, and 14; Figures S1 and S2 in Supporting Information S1), which indicates that some mechanisms have a greater likelihood for producing large floods than others (Tarasova et al., 2020). Detailed mechanistic studies of all floods in parts of Regions 14 and 3 by Collins et al. (2014) and Hirschboeck (1987), respectively, show how the relatively wide range of synoptic storm types, precipitation mechanisms, and antecedent conditions that produce floods in these areas often have different seasonal timing and are not necessarily equal in their flood magnitude potential.

For example, Collins et al. (2014) identified the synoptic storm types, seasonality, and precipitation mechanisms for all AMS floods from 1949 to 2006 for 10 streamgages in the Northeast United States with near-natural streamflow, eight of which are in Region 14 (Northeast). We reanalyzed their data to segregate attributions for

Table 2
Relationships Between Annual Counts of Large Floods and Climate Indices for the Period 1966–2015 for All of the Conterminous United States (CONUS) and the 14 Regions

		CONUS	Regions													
			1	2	3	4	5	6	7	8	9	10	11	12	13	14
2 Largest																
AMO	<i>p</i> -value	0.55	0.85	0.98	0.99	0.47	0.30	0.91	0.08	0.45	0.47	0.06	0.84	0.86	0.33	0.48
	Trend	−4.38	0.38	0.04	−0.01	0.83	−0.75	−0.07	−2.08	−0.60	−0.61	−1.26	0.19	0.08	−2.14	1.53
NAO	<i>p</i> -value	0.48	0.25	0.35	0.27	0.03	0.09	0.17	0.07	0.38	0.06	0.73	0.89	0.87	0.25	0.24
	Trend	−6.37	2.40	−1.66	−0.87	−3.10	−1.64	−1.08	2.38	0.78	1.85	−0.26	0.14	0.10	−3.19	−3.20
PDO	<i>p</i> -value	0.78	0.86	0.10	0.35	0.84	0.61	0.30	0.73	1.00	0.17	0.56	0.38	0.87	0.85	0.57
	Trend	2.17	0.39	2.36	0.65	−0.27	−0.41	0.69	0.45	0.00	−1.27	0.38	0.83	0.08	−0.45	−1.37
PNA	<i>p</i> -value	0.08	0.33	0.99	0.32	0.40	0.099	0.45	0.67	0.92	0.56	0.002	0.07	0.65	0.04	0.34
	Trend	−15.37	−2.47	0.02	0.77	1.18	−1.49	−0.60	−0.62	−0.10	−0.60	−2.89	−2.19	0.25	−5.47	−2.70
ENSO	<i>p</i> -value	0.40	0.20	0.10	0.37	0.05	0.42	0.07	0.46	0.86	0.33	0.62	0.48	0.71	0.79	0.08
	Trend	−7.23	−3.05	2.54	0.68	−2.88	−0.70	1.29	1.00	0.16	−1.00	−0.36	−0.78	0.20	−0.72	−4.48
10 Largest																
AMO	<i>p</i> -value	0.77	0.62	0.75	0.64	0.98	0.68	0.97	0.33	0.97	0.61	0.03	0.38	0.12	0.42	0.35
	Trend	−5.04	−2.18	1.51	−0.92	−0.09	0.87	−0.06	−3.25	−0.07	−1.11	−3.23	1.68	2.11	−4.87	4.61
NAO	<i>p</i> -value	0.51	0.88	0.18	0.99	0.13	0.39	0.75	0.35	0.25	0.06	0.55	0.47	0.73	0.96	0.24
	Trend	−13.77	−0.80	−7.87	0.03	−6.24	−2.20	−0.71	3.76	2.37	4.64	−1.10	1.64	−0.59	−0.35	−7.18
PDO	<i>p</i> -value	0.22	0.45	0.08	0.15	0.74	0.90	0.20	0.76	0.42	0.90	0.64	0.52	0.40	0.26	0.61
	Trend	23.06	−3.75	8.45	2.99	1.24	0.30	2.51	1.12	−1.57	−0.29	−0.76	1.33	1.29	7.27	2.78
PNA	<i>p</i> -value	0.51	0.13	0.65	0.34	0.96	0.98	0.79	0.71	0.67	0.50	<0.001	0.23	0.15	0.27	0.94
	Trend	−14.12	−8.53	2.49	2.23	0.21	0.06	0.60	1.51	−0.93	1.77	−6.91	−2.90	2.37	−8.08	0.44
ENSO	<i>p</i> -value	0.74	0.16	0.07	0.04	0.22	1.00	0.01	0.16	0.66	0.95	0.22	0.34	0.07	0.71	0.31
	Trend	6.91	−7.68	9.35	4.70	−5.09	−0.01	5.55	5.45	−0.90	−0.18	−2.25	−2.18	2.96	2.61	−5.92

Note. Trend values are changes in annual flood counts over the range of a given index, as computed by quasi-Poisson regression. Bold *p*-values are significant at $p < 0.1$. Atlantic Multidecadal Oscillation (AMO), North Atlantic Oscillation (NAO), Pacific Decadal Oscillation (PDO), Pacific North American pattern (PNA), and El Niño–Southern Oscillation (ENSO).

the 10 largest and 2 largest floods and compared them to those for all AMS floods. Table 3 shows that as flood magnitudes increase in Region 14 going from all AMS floods to the 2 largest, the relative importance of the June–July–August (JJA) and September–October–November (SON) periods increases as indicated by increasing percent occurrence of events. This is also reflected in precipitation mechanism changes: the relative importance of rain increases with flood magnitude while rain–snowmelt decreases.

The seasonality change reflects important changes in synoptic storm types. As floods get larger, two synoptic storm types in particular become more important: coastal lows and tropical cyclones (Table 3). Both storm types can generate rainfall rates and/or durations sufficient to produce large floods at a time of year that typically has low antecedent soil moisture and is generally flood-poor for smaller, more frequent events (Collins, 2019). Coastal lows are most common in Region 14 in the cold season (October–April), but they can occur any time of year (Agel et al., 2015; Davis et al., 1993; Hirsch et al., 2001). Reanalysis of the Collins et al. (2014) data set shows that coastal lows account for about half of the 10 largest and 2 largest floods that occur in June (not shown). Agel et al. (2019) also demonstrated the importance of coastal lows for generating large floods in eastern Massachusetts, the majority of which occur from February through June. Coastal lows are associated with larger floods in Region 14 because they access Atlantic Ocean moisture and their orientations with respect to the Appalachian Mountains can provide opportunities for orographic enhancement (Agel et al., 2019; Collins et al., 2014; Smith et al., 2011). The Collins et al. (2014) data set shows that tropical cyclones strongly influence large-flood occurrence in Region 14 in August and September, similar to the findings of Agel et al. (2019). These powerful storms

Table 3
Attributions of Annual Maximum Flood Events by Collins et al. (2014) for 10 New England Streams With Near-Natural Flood Conditions (1949–2006)

	All AMS	10 Largest	2 Largest
Synoptic storm type			
Great Lakes low	252 (0.44)	42 (0.42)	7 (0.35)
Coastal low	122 (0.21)	24 (0.24)	6 (0.30)
Ohio Valley low	86 (0.15)	16 (0.16)	3 (0.15)
Canada low	16 (0.03)	0 (0.00)	0 (0.00)
Multiple lows	38 (0.07)	7 (0.07)	1 (0.05)
Tropical cyclone	28 (0.05)	6 (0.06)	2 (0.10)
Other	35 (0.06)	5 (0.05)	1 (0.05)
<i>Total</i>	577 (1.00)	100 (1.00)	20 (1.00)
Season (months)			
MAM	357 (0.62)	58 (0.58)	11 (0.55)
DJF	108 (0.19)	15 (0.15)	1 (0.05)
SON	76 (0.13)	15 (0.15)	5 (0.25)
JJA	36 (0.06)	12 (0.12)	3 (0.15)
<i>Total</i>	577 (1.00)	100 (1.00)	20 (1.00)
Precipitation mechanism			
Rain	410 (0.74)	73 (0.78)	16 (0.84)
Rain-snowmelt	109 (0.20)	12 (0.13)	2 (0.11)
ROS	29 (0.05)	7 (0.07)	1 (0.05)
Snowmelt	8 (0.01)	2 (0.02)	0 (0.00)
<i>Total</i>	556 (1.00)	94 (1.00)	19 (1.00)

Note. Eight of the ten are also in Region 14 of this study. We reanalyzed their data to evaluate attributions for the 10 largest and the 2 largest floods. Numbers in parentheses show the relative proportions of events per attribution category. The number of floods classifiable for precipitation mechanisms was limited by station availability.

are characterized by ample water vapor and the precipitation they generate can be orographically enhanced in Region 14 (Smith et al., 2010).

Detailed regional studies that identify flood-generating mechanisms that are more likely to produce large floods can help communities better understand and prepare for the most consequential events (e.g., Agel et al., 2019; Barth et al., 2017; Neiman et al., 2011; Tarasova et al., 2020). Regions with different seasonality for large floods and all AMS floods (e.g., the Northwest [Region 1], Mid-Atlantic [13] and Northeast [14]) are areas where these kinds of analyses may be particularly helpful to communities for identifying the conditions they should be most concerned about.

4.2. Changes Over Time, 1966–2015

Using quasi-Poisson regression, our study found insignificant decreases in the annual numbers of the 2 largest and 10 largest floods for the entire CONUS from 1966 to 2015, for basins that are minimally altered with flood flows that are expected to be sensitive only to climatic change and variability. Our novel method based on expected occurrence had similar findings. Across CONUS, observed frequencies of the 2 largest and 10 largest floods in the most recent 25 and 10 yr periods of the record were generally no different from the expected frequencies. Our occurrence results for the entire CONUS are consistent with previous national studies of POT floods, which include many small floods that do not overflow riverbanks (Archfield et al., 2016; Hodgkins et al., 2019).

National trends in the annual numbers of the 2 largest and 10 largest floods found here are also consistent with results from Hodgkins et al. (2017). They analyzed trends in the annual occurrence of major floods (exceeding

25, 50, and 100 yr thresholds) in North America and Europe for minimally altered basins. Their regions were much larger than ours, with 3 regions in North America compared to 14 across CONUS for this study. Hodgkins et al. (2017) found no significant trends in major-flood occurrence from 1961 to 2010 for their 3 regions. Unlike the current study, they did not analyze seasonal flood trends.

Despite a lack of national trends, our regression analyses identified one region with a significant negative trend for the 2 largest floods, Region 7 (Gulf Coast), and two regions with significant trends for the 10 largest floods (Table 1 and Figures 7 and 8). Region 7 had a significant negative trend for the 10 largest floods as it did for the 2 largest floods, and Region 11 (Ohio River Basin) had a significant positive trend. Our novel method based on expected occurrence corroborated these results. The southeast, particularly Louisiana, had aggregations of stations that showed 3 or less 10 largest floods in the latter half of the record (Figure 4b) and zero 10 largest floods in the last 10 yr of record (Figure 5b). The Ohio River Basin had a cluster of stations that recorded 7 or more of their 10 largest floods in the latter half of the record (Figure 4c) and 4, 5, or 6 of their 10 largest floods in the last 10 yr of record (Figure 5b). Although no other regions showed significant trends for the 10 largest floods via quasi-Poisson regression, spatial aggregations of streamgages with unusually low or high counts of the 10 largest floods in later periods of the record (Figures 4b, 4c, and 5b) often show the same direction of change as the trend magnitude for the corresponding region (Figure 8).

Dethier et al. (2020) examined historical trends in 2 to 25 yr floods in North America for annual and seasonal floods; they found many significant regional increases and no significant decreases from 1950 to 2016 for selected seasons (winter, spring, summer, and fall). For annual periods, they found significant trends in floods for multiple recurrence intervals for multiple regions. The higher percentage of regions with significant flood increases in Dethier et al. (2020) as compared to our study is likely due to different time periods considered. Hodgkins et al. (2019), examining trends in U.S. POT that occurred on average once in five years, found more minimally altered basins with significant annual peak-flow increases (12.2%) for the 1941–2015 period than for the 1966–2015 period (3.4%). Hodgkins et al. (2017) found significant increases in the number of 25 yr floods in North America (mostly in CONUS) from 1931 to 2010 but an insignificant change from 1961 to 2010. Ryberg et al. (2020) found that many gages across CONUS had a change point (step change) toward higher magnitude annual peak flows around 1970.

4.3. Relations Between Large-Flood Occurrence and Climate Indices

In contrast to the lack of significant 2 largest flood trends for CONUS from 1966 to 2015, there was a significant negative relation between the number of the 2 largest floods and the PNA at the national scale, though the amount of explained interannual variance was very low at 5.9%. This negative relation was significant for Region 10 (Upper Midwest) for both the 2 largest and 10 largest floods with explained variance of 17.4% and 22.9%, respectively. This is likely because there is large moisture transport leading to an increased number of heavy rainfall events and flooding in all seasons during the negative phase of PNA in the north-central United States (Mallakpour & Villarini, 2016). Archfield et al. (2016) found that the number of peaks over threshold was significantly related to PNA at 20% of basins in CONUS. These results suggest that the PNA influences the occurrence of large and small floods to varying degrees across CONUS.

ENSO had significant positive relations with the annual number of 10 largest floods for three contiguous regions from California to Texas, with low explained variance (6.1%–13.7%). This is consistent with previous work (Pizarro & Lall, 2002) that found ENSO had significant positive relations with annual maximum floods at many basins in the southwestern United States, suggesting ENSO influences large and small floods in this area of CONUS. A positive ENSO phase is associated with widespread increased precipitation (especially in winter months) in the southwest, southeast, and central United States (Anderson & Emmanuel, 2008; McCabe & Dettinger, 1999; Ropelewski & Halpert, 1986).

4.4. Key Assumptions and Data Limitations

Large floods are less frequently studied than AMS floods, partly because their rarity presents sample size constraints. One way we addressed this was by pooling data into climatic/physiographic regions. We adopted regions defined by McCabe and Wolock (2014), but these were identified based on annual mean flow regimes. We assume these regions also meaningfully distinguish flood behavior, which seems reasonable given their coherence

with climatic/physiographic regions across CONUS and the correspondence between our seasonality results and those of regional studies of large floods in Regions 1 and 14 (Agel et al., 2019; Neiman et al., 2011).

Although we examined nested basins as a basis to remove some spatially correlated streamgages from the analyses (see Section 2.1), we did not explicitly consider spatial correlation for non-nested streamgages. Our quasi-Poisson regression method is robust to spatial correlation and other factors because of the use of a dispersion index (Hodgkins et al., 2017), but our method based on expected values and the approach to identifying flood-rich months (seasons) could be affected. Since our expected value results are similar to the quasi-Poisson results, we think any impact on that method is minimal. Spatial correlation could affect our identification of flood seasons by reducing the effective number of observations in a region, thus producing confidence intervals that are too narrow and increasing the likelihood that we too permissively identify a flood-rich month (season). However, we think the actual impacts are limited because, as noted above, we have good correspondence between our seasonality results in regions where there are also large-flood seasonality studies of individual stations (e.g., Agel et al., 2019; Neiman et al., 2011). Moreover, the consequence of any effect—analysis of a “significant” flood season that is not actually significant—is small.

Our analyses are limited by record length and basin size. As with all studies of near-natural flood conditions, our study basins are relatively small (generally <2,000 km²) and may not well represent hydroclimatic conditions and flood-generating mechanisms in large basins. Furthermore, because we used AMS records to identify the 10 largest floods for the period of record at our sites, it is possible that we did not capture what were truly the 10 largest floods at a given site. AMS time series include only the largest event of each year, so sites that had years with more than one flood greater than the 10th largest AMS flood would record only the largest of them.

5. Conclusions

Large floods are defined in our study as the 10 largest AMS floods observed at a station over the 50 yr study period from water year 1966 through water year 2015. These are typically overbank floods at a given site with recurrence intervals ranging from about 5 to 50 yr. We repeated most analyses using only the 2 largest AMS floods in the same period at each station. Overbank floods have important ecological functions, but they also pose risks to floodplain infrastructure and human communities. Understanding when large floods occur during the year, if their occurrence is changing, and the mechanisms that generate them can help communities plan for, and respond to, these events. Our study provides the first detailed characterization of large-flood seasonality across CONUS, and we evaluate changes in their occurrence over a period of time that is predominantly after 1970 when an important hydroclimatic shift occurred in the study area (Ryberg et al., 2020). Our seasonal characterizations provide an entry point for other studies to develop detailed understanding of regional flood-generating processes.

The seasonality of large floods in the modern hydroclimatic regime varies considerably across the country. Some regions have highly seasonal monthly frequency distributions with occurrence concentrated in a handful of contiguous months. Other regions have more complex, or weak, large-flood seasonality with monthly frequency distributions that are multi-modal or have little pronounced modality. Regions where large floods have complex seasonality may have numerous flood-generating mechanisms and these may have different potentials for producing large floods (e.g., the Northeast; Collins et al., 2014). On the other hand, we infer that regions with strong seasonality have fewer flood-generating mechanisms (e.g., the Northwest; Barth et al., 2017; Neiman et al., 2011), but more studies are needed to confirm our inferences.

Using two complementary approaches, including a novel and generalizable method based on expected occurrence, we did not find evidence for strong and consistent changes in the frequency of large floods across CONUS in the modern hydroclimate regime (1966–2015). Only two of fourteen regions showed significant trends over time in annual counts of the 10 largest floods (of opposite sign) and one region showed a significant decrease in the occurrence of the 2 largest floods. Seasonal analyses by region also had few significant trends. These results, found by quasi-Poisson regression, were corroborated by our novel method and were broadly similar to results of earlier trend studies of AMS floods that considered a similar period.

The PNA stands out as a mode of climate variability that is significantly related to the occurrence of the 2 largest floods across CONUS, and is strongly associated with the 2 largest and 10 largest floods in part of the Upper Midwest. ENSO also is significantly related to the 10 largest floods from California to Texas, and in Florida.

Other indices of climate variability that we evaluated show only a limited number of regional relationships with large floods.

Although a few past studies focusing on large floods in North America have found climate-associated trends in occurrence over time, these trends were based on longer periods of record. We find that large-flood occurrence across CONUS has generally been stable in the modern hydroclimate period that began around 1970. Whether that continues with projected changes in climate remains to be seen.

Data Availability Statement

All discharge time series at USGS streamgages are freely available at: <http://dx.doi.org/10.5066/F7P55KJN>. The data that support the findings of this study are in an associated USGS data release (Archfield et al., 2022).

Acknowledgments

The authors thank Caelan Simeone for quality assurance and graphics support. An earlier version of the manuscript was improved considerably by feedback from John Hammond and four anonymous reviewers.

References

- Agel, L., Barlow, M., Collins, M. J., Douglas, E., & Kirshen, P. (2019). Hydrometeorological conditions preceding extreme streamflow for the Charles and Mystic River Basins of Eastern Massachusetts. *Journal of Hydrometeorology*, 20(9), 1795–1812. <https://doi.org/10.1175/JHM-D-19-0017.1>
- Agel, L., Barlow, M., Qian, J. H., Colby, F., Douglas, E., & Eichler, T. (2015). Climatology of daily precipitation and extreme precipitation events in the Northeast United States. *Journal of Hydrometeorology*, 16(6), 2537–2557. <https://doi.org/10.1175/JHM-D-14-0147.1>
- Ahn, K. H., & Palmer, R. N. (2016). Trend and variability in observed hydrological extremes in the United States. *Journal of Hydrologic Engineering*, 21(2), 04015061. [https://doi.org/10.1061/\(asce\)he.1943-5584.0001286](https://doi.org/10.1061/(asce)he.1943-5584.0001286)
- Anderson, W. P., & Emmanuel, R. E. (2008). Effect of interannual and interdecadal climate oscillations on groundwater in North Carolina. *Geophysical Research Letters*, 35, L23402. <https://doi.org/10.1029/2008GL036054>
- Archfield, S. A., Collins, M. J., & Hodgkins, G. A. (2022). Ten largest annual instantaneous floods and seasonal signal for reference streamgages in the United States, water years 1966–2015. U.S. Geological Survey data release. <https://doi.org/10.5066/P9QYR28M>
- Archfield, S. A., Hirsch, R. M., Viglione, A., & Blöschl, G. (2016). Fragmented patterns of flood change across the United States. *Geophysical Research Letters*, 43(19), 10232–10239. <https://doi.org/10.1002/2016GL070590>
- Armstrong, W. H., Collins, M. J., & Snyder, N. P. (2014). Hydroclimatic flood trends in the Northeastern United States and linkages with large-scale atmospheric circulation patterns. *Hydrological Sciences Journal*, 59, 1636–1655. <https://doi.org/10.1080/02626667.2013.862339>
- Ashley, S. T., & Ashley, W. S. (2008). Flood fatalities in the United States. *Journal of Applied Meteorology and Climatology*, 47, 805–818. <https://doi.org/10.1175/2007JAMC1611.1>
- Barth, N. A., Villarini, G., Nayak, M. A., & White, K. (2017). Mixed populations and annual flood frequency estimates in the western United States: The role of atmospheric rivers. *Water Resources Research*, 53(1), 257–269. <https://doi.org/10.1002/2016WR019064>
- Berghuijs, W. R., Woods, R. A., Hutton, C. J., & Sivapalan, M. (2016). Dominant flood generating mechanisms across the United States. *Geophysical Research Letters*, 43(9), 4382–4390. <https://doi.org/10.1002/2016GL068070>
- Bertola, M., Viglione, A., Lun, D., Hall, J., & Blöschl, G. (2020). Flood trends in Europe: Are changes in small and big floods different? *Hydrology and Earth System Sciences*, 24(4), 1805–1822. <https://doi.org/10.5194/hess-24-1805-2020>
- Blöschl, G., Hall, J., Parajka, J., Perdigão, R. A., Merz, B., Arheimer, B., et al. (2017). Changing climate shifts timing of European floods. *Science*, 357(6351), 588–590. <https://doi.org/10.1126/science.aan2506>
- Blöschl, G., Hall, J., Viglione, A., Perdigão, R. A., Parajka, J., Merz, B., et al. (2019). Changing climate both increases and decreases European river floods. *Nature*, 573(7772), 108–111. <https://doi.org/10.1038/s41586-019-1495-6>
- Burn, D. H., & Whitfield, P. H. (2016). Changes in floods and flood regimes in Canada. *Canadian Water Resources Journal*, 41(1–2), 139–150. <https://doi.org/10.1080/07011784.2015.1026844>
- Burn, D. H., Whitfield, P. H., & Sharif, M. (2016). Identification of changes in floods and flood regimes in Canada using a peak over threshold approach. *Hydrological Processes*, 30(18), 3303–3314. <https://doi.org/10.1002/hyp.10861>
- Collins, M. J. (2009). Evidence for changing flood risk in New England since the late 20th century. *Journal of the American Water Resources Association*, 45(2), 279–290. <https://doi.org/10.1111/j.1752-1688.2008.00277.x>
- Collins, M. J. (2019). River flood seasonality in the Northeast United States: Characterization and trends. *Hydrological Processes*, 33(5), 687–698. <https://doi.org/10.1002/hyp.13355>
- Collins, M. J., Kirk, J. P., Pettit, J., DeGaetano, A. T., McCown, M. S., Peterson, T. C., et al. (2014). Annual floods in New England (USA) and Atlantic Canada: Synoptic climatology and generating mechanisms. *Physical Geography*, 35(3), 195–219. <https://doi.org/10.1080/02723646.2014.888510>
- Costa, J. E. (1987). Hydraulics and basin morphometry of the largest flash floods in the conterminous United States. *Journal of Hydrology*, 93(3–4), 313–338. [https://doi.org/10.1016/0022-1694\(87\)90102-8](https://doi.org/10.1016/0022-1694(87)90102-8)
- Crippen, J. R., & Bue, C. D. (1977). *Maximum flood flows in the conterminous United States. U.S. Geol. Survey Water Supply Paper 1887* (p. 52).
- Cunderlik, J. M., Ouarda, T. B. M. J., & Bobée, B. (2004). On the objective identification of flood seasons. *Water Resources Research*, 40, W01520. <https://doi.org/10.1029/2003WR002295>
- Davis, R. E., Dolan, R., & Demme, G. (1993). Synoptic climatology of Atlantic coast North-Easterners. *International Journal of Climatology*, 13(2), 171–189. <https://doi.org/10.1002/joc.3370130204>
- Dethier, E. N., Sartain, S. L., Renshaw, C. E., & Magilligan, F. J. (2020). Spatially coherent regional changes in seasonal extreme streamflow events in the United States and Canada since 1950. *Science Advances*, 6(49), eaba5939. <https://doi.org/10.1126/sciadv.aba5939>
- Dickinson, J. E., Harden, T. M., & McCabe, G. J. (2019). Seasonality of climatic drivers of flood variability in the conterminous United States. *Scientific Reports*, 9(1), 1–10. <https://doi.org/10.1038/s41598-019-51722-8>
- Douglas, E. M., Vogel, R. M., & Kroll, C. N. (2000). Trends in floods and low flows in the United States: Impact of spatial correlation. *Journal of Hydrology*, 240(1–2), 90–105. [https://doi.org/10.1016/S0022-1694\(00\)00336-X](https://doi.org/10.1016/S0022-1694(00)00336-X)

- Dudley, R. W., Archfield, S. A., Hodgkins, G. A., Renard, B., & Ryberg, K. R. (2018). *Basin characteristics and peak-streamflow trends and change-points for 2,683 USGS streamgages in the conterminous U.S.* U.S. Geological Survey Data Release. <https://doi.org/10.5066/P9AEGXY0>
- Enfield, D. B., Mestas-Núñez, A. M., & Trimble, P. J. (2001). The Atlantic multidecadal oscillation and its relation to rainfall and river flows in the continental US. *Geophysical Research Letters*, 28(10), 2077–2080. <https://doi.org/10.1029/2000GL012745>
- England, J. F., Jr, Cohn, T. A., Faber, B. A., Stedinger, J. R., Thomas, W. O., Jr, Veilleux, A. G., et al. (2019). *Guidelines for determining flood flow frequency—Bulletin 17C: U.S. Geological Survey Techniques and Methods.* (book 4, chap. B5, p. 148). <https://doi.org/10.3133/tm4B5>
- Falcone, J. A. (2011). GAGES—II—Geospatial attributes of gages for evaluating streamflow. U.S. Geological Survey Metadata. Retrieved from http://water.usgs.gov/GIS/metadata/usgswrd/XML/gagesII_Sept2011.xml
- Frome, E. L., & Checkoway, H. (1985). Use of Poisson regression models in estimating incidence rates and ratios. *American Journal of Epidemiology*, 121(2), 309–323. <https://doi.org/10.1093/oxfordjournals.aje.a114001>
- Hirsch, M. E., DeGaetano, A. T., & Colucci, S. J. (2001). An East Coast winter storm climatology. *Journal of Climate*, 14, 882–899. [https://doi.org/10.1175/1520-0442\(2001\)014<0882:AECWSC>2.0.CO;2](https://doi.org/10.1175/1520-0442(2001)014<0882:AECWSC>2.0.CO;2)
- Hirschboeck, K. K. (1987). Hydroclimatically defined mixed distributions in partial duration flood series. In *Hydrologic frequency modeling* (pp. 199–212). Springer. https://doi.org/10.1007/978-94-009-3953-0_13
- Hirschboeck, K. K. (1991). Climate and floods. In R. W. Paulson, E. B. Chase, & D. W. Moody (Eds.), *National water summary 1988–89, floods and droughts* (p. 2375). US Geol. Surv. Water Supply
- Hodgkins, G. A., Dudley, R. W., Archfield, S. A., & Renard, B. (2019). Effects of climate, regulation, and urbanization on historical flood trends in the United States. *Journal of Hydrology*, 573, 697–709. <https://doi.org/10.1016/j.jhydrol.2019.03.102>
- Hodgkins, G. A., Whitfield, P. H., Burn, D. H., Hannaford, J., Renard, B., Stahl, K., et al. (2017). Climate-driven variability in the occurrence of major floods across North America and Europe. *Journal of Hydrology*, 552, 704–717. <https://doi.org/10.1016/j.jhydrol.2017.07.027>
- Hurrell, J. W., Kushnir, Y., Ottensen, G., & Visbeck, M. (2003). *An overview of the North Atlantic Oscillation* (Vol. 134, pp. 1–35). Geophysical Monograph—American Geophysical Union. <https://doi.org/10.1029/134gm01>
- Hurrell, J. W., & Van Loon, H. (1997). Decadal variations in climate associated with the North Atlantic Oscillation. In *Climatic change at high elevation sites* (pp. 69–94). Dordrecht: Springer. https://doi.org/10.1007/978-94-015-8905-5_4
- Junk, W. J., Bayley, P. B., & Sparks, R. E. (1989). The flood pulse concept in river-floodplain systems. *Canadian Special Publication of Fisheries and Aquatic Sciences*, 106(1), 110–127.
- Leathers, D. J., & Palecki, M. A. (1992). The Pacific/North American teleconnection pattern and United States climate. Part II: Temporal characteristics and index specification. *Journal of Climate*, 5(7), 707–716. [https://doi.org/10.1175/1520-0442\(1992\)005<0707:TPATPA>2.0.CO;2](https://doi.org/10.1175/1520-0442(1992)005<0707:TPATPA>2.0.CO;2)
- Lins, H. F. (2012). USGS hydro-climatic data network 2009 (HCDN–2009). U.S. Geological Survey Fact Sheet 2012–3047, 4 p. Retrieved from <https://pubs.usgs.gov/fs/2012/3047/>
- Lins, H. F., & Slack, J. R. (1999). Streamflow trends in the United States. *Geophysical Research Letters*, 26(2), 227–230. <https://doi.org/10.1029/1998GL900291>
- Lins, H. F., & Slack, J. R. (2005). Seasonal and regional characteristics of US streamflow trends in the United States from 1940 to 1999. *Physical Geography*, 26(6), 489–501. <https://doi.org/10.2747/0272-3646.26.6.489>
- Lun, D., Fischer, S., Viglione, A., & Blöschl, G. (2020). Detecting flood-rich and flood-poor periods in annual peak discharges across Europe. *Water Resources Research*, 56, e2019WR026575. <https://doi.org/10.1029/2019wr026575>
- Lytle, D. A., & Poff, N. L. (2004). Adaptation to natural flow regimes. *Trends in Ecology & Evolution*, 19(2), 94–100. <https://doi.org/10.1016/j.tree.2003.10.002>
- Mallakpour, I., & Villarini, G. (2015). The changing nature of flooding across the central United States. *Nature Climate Change*, 5(3), 250–254. <https://doi.org/10.1038/nclimate2516>
- Mallakpour, I., & Villarini, G. (2016). Investigating the relationship between the frequency of flooding over the central United States and large-scale climate. *Advances in Water Resources*, 92, 159–171. <https://doi.org/10.1016/j.advwatres.2016.04.008>
- Mantua, N. J., & Hare, S. R. (2002). The Pacific Decadal Oscillation. *Journal of Oceanography*, 58(1), 35–44. <https://doi.org/10.1023/A:1015820616384>
- Mardia, K. V. (1972). *Statistics of directional data*. New York, NY: Academic Press.
- McCabe, G. J., & Dettinger, M. D. (1999). Decadal variations in the strength of ENSO teleconnections with precipitation in the western United States. *International Journal of Climatology*, 19(13), 1399–1410. [https://doi.org/10.1002/\(SICI\)1097-0088\(19991115\)19:13<1399::AID-JOC457>3.0.CO;2-A](https://doi.org/10.1002/(SICI)1097-0088(19991115)19:13<1399::AID-JOC457>3.0.CO;2-A)
- McCabe, G. J., & Wolock, D. M. (2002). A step increase in streamflow in the conterminous United States. *Geophysical Research Letters*, 29(24), 38-1–38-4. <https://doi.org/10.1029/2002GL015999>
- McCabe, G. J., & Wolock, D. M. (2014). Spatial and temporal patterns in conterminous United States streamflow characteristics. *Geophysical Research Letters*, 41(19), 6889–6897. <https://doi.org/10.1002/2014GL061980>
- McCullagh, P., & Nelder, J. A. (1989). *Generalized linear models* (2nd ed.). Boca Raton, FL: CRC Press.
- Mediero, L., Kjeldsen, T. R., Macdonald, N., Kohnova, S., Merz, B., Vorogushyn, S., et al. (2015). Identification of coherent flood regions across Europe by using the longest streamflow records. *Journal of Hydrology*, 528, 341–360. <https://doi.org/10.1016/j.jhydrol.2015.06.016>
- Milly, P. C. D., Wetherald, R. T., Dunne, K. A., & Delworth, T. L. (2002). Increasing risk of great floods in a changing climate. *Nature*, 415, 514–517. <https://doi.org/10.1038/415514a>
- National Oceanic and Atmospheric Administration (NOAA) (2019). Retrieved from <http://www.esrl.noaa.gov/psd/data/timeseries/AMO/>
- Neiman, P. J., Schick, L. J., Ralph, F. M., Hughes, M., & Wick, G. A. (2011). Flooding in western Washington: The connection to atmospheric rivers. *Journal of Hydrometeorology*, 12(6), 1337–1358. <https://doi.org/10.1175/2011JHM1358.1>
- NOAA (2020a). Retrieved from <https://www.ncdc.noaa.gov/teleconnections/nao/>
- NOAA (2020b). Retrieved from <https://www.ncdc.noaa.gov/teleconnections/pdo/>
- NOAA (2020c). Retrieved from <https://www.ncdc.noaa.gov/teleconnections/pna/>
- NOAA (2020d). Retrieved from <http://www.esrl.noaa.gov/psd/data/climateindices/>
- NOAA National Centers for Environmental Information (NCEI). (2021). *U.S. billion-dollar weather and climate disasters*. <https://doi.org/10.25921/stkw-7w73>
- Nussbaum, E. M., Elsadat, S., & Khago, A. H. (2008). Best practices in analyzing count data: Poisson regression. *Best practices in quantitative methods* (pp. 306–323).
- O'Connor, J. E., & Costa, J. E. (2004). Spatial distribution of the largest rainfall-runoff floods from basins between 2.6 and 26,000 km² in the United States and Puerto Rico. *Water Resources Research*, 40(1), W01107. <https://doi.org/10.1029/2003WR002247>

- Petrow, T., & Merz, B. (2009). Trends in flood magnitude, frequency, and seasonality in Germany in the period 1951–2002. *Journal of Hydrology*, 371(1–4), 129–141. <https://doi.org/10.1016/j.jhydrol.2009.03.024>
- Pizarro, G., & Lall, U. (2002). El Niño-induced flooding in the US West: What can we expect? *Eos Transactions American Geophysical Union*, 83(32), 349–352. <https://doi.org/10.1029/2002EO000255>
- Poff, N. L., Allan, J. D., Bain, M. B., Karr, J. R., Prestegard, K. L., Richter, B. D., et al. (1997). The natural flow regime. *BioScience*, 47(11), 769–784. <https://doi.org/10.2307/1313099>
- R Core Team. (2019). *R: A language and environment for statistical computing*. Vienna, Austria: R Foundation for Statistical Computing. Retrieved from <https://www.R-project.org/>
- Ropelewski, C. F., & Halpert, M. S. (1986). North American precipitation and temperature patterns associated with the El Niño/Southern Oscillation (ENSO). *Monthly Weather Review*, 114(12), 2352–2362. [https://doi.org/10.1175/1520-0493\(1986\)114<2352:NAPATP>2.0.CO;2](https://doi.org/10.1175/1520-0493(1986)114<2352:NAPATP>2.0.CO;2)
- Ryberg, K. R., Hodgkins, G. A., & Dudley, R. W. (2020). Change points in annual peak streamflows: Method comparisons and historical change points in the United States. *Journal of Hydrology*, 583, 124307. <https://doi.org/10.1016/j.jhydrol.2019.124307>
- Slater, L., Villarini, G., Archfield, S., Faulkner, D., Lamb, R., Khouakhi, A., & Yin, J. (2021). Global changes in 20, 50, and 100 yr river floods. *Geophysical Research Letters*, 48, e2020GL091824. <https://doi.org/10.1029/2020GL091824>
- Smith, A. B., & Katz, R. W. (2013). US billion-dollar weather and climate disasters: Data sources, trends, accuracy and biases. *Natural Hazards*, 67(2), 387–410. <https://doi.org/10.1007/s11069-013-0566-5>
- Smith, J. A., & Baeck, M. L. (2015). “Prophetic vision, vivid imagination”: The 1927 Mississippi River flood. *Water Resources Research*, 51, 9964–9994. <https://doi.org/10.1002/2015WR017927>
- Smith, J. A., Baeck, M. L., Villarini, G., & Krajewski, W. F. (2010). The hydrology and hydrometeorology of flooding in the Delaware River Basin. *Journal of Hydrometeorology*, 11(4), 841–859. <https://doi.org/10.1175/2010JHM1236.1>
- Smith, J. A., Baeck, M. L., Yang, L., Signell, J., Morin, E., & Goodrich, D. C. (2019). The paroxysmal precipitation of the desert: Flash floods in the Southwestern United States. *Water Resources Research*, 55(12), 10218–10247. <https://doi.org/10.1029/2019WR025480>
- Smith, J. A., Cox, A. A., Baeck, M. L., Yang, L., & Bates, P. (2018). Strange floods: The upper tail of flood peaks in the United States. *Water Resources Research*, 54(9), 6510–6542. <https://doi.org/10.1029/2018WR022539>
- Smith, J. A., Villarini, G., & Baeck, M. L. (2011). Mixture distributions and the hydroclimatology of extreme rainfall and flooding in the eastern United States. *Journal of Hydrometeorology*, 12, 294–309. <https://doi.org/10.1175/2010JHM1242.1>
- Tarasova, L., Basso, S., & Merz, R. (2020). Transformation of generation processes from small runoff events to large floods. *Geophysical Research Letters*, 47(22), e2020GL090547. <https://doi.org/10.1029/2020GL090547>
- Tootle, G. A., Piechota, T. C., & Singh, A. (2005). Coupled oceanic-atmospheric variability and US streamflow. *Water Resources Research*, 41(12). <https://doi.org/10.1029/2005WR004381>
- U.S. Geological Survey. (2020). National Water Information System data available on the World Wide Web (USGS Water Data for the Nation). <https://doi.org/10.5066/F7P55KJN>
- Villarini, G. (2016). On the seasonality of flooding across the continental United States. *Advances in Water Resources*, 87, 80–91. <https://doi.org/10.1016/j.advwatres.2015.11.009>
- Villarini, G., Goska, R., Smith, J. A., & Vecchi, G. A. (2014). North Atlantic tropical cyclones and US flooding. *Bulletin of the American Meteorological Society*, 95(9), 1381–1388. <https://doi.org/10.1175/BAMS-D-13-00060.1>
- Villarini, G., Serinaldi, F., Smith, J. A., & Krajewski, W. F. (2009). On the stationarity of annual flood peaks in the continental United States during the 20th century. *Water Resources Research*, 45(8). <https://doi.org/10.1029/2008WR007645>
- Villarini, G., & Smith, J. A. (2010). Flood peak distributions for the eastern United States. *Water Resources Research*, 46(6), W06504. <https://doi.org/10.1029/2009WR008395>
- Villarini, G., Smith, J. A., Serinaldi, F., & Ntelekos, A. A. (2011). Analyses of seasonal and annual maximum daily discharge records for central Europe. *Journal of Hydrology*, 399(3–4), 299–312. <https://doi.org/10.1016/j.jhydrol.2011.01.007>
- Villarini, G., Smith, J. A., Serinaldi, F., Ntelekos, A. A., & Schwarz, U. (2012). Analyses of extreme flooding in Austria over the period 1951–2006. *International Journal of Climatology*, 32(8), 1178–1192. <https://doi.org/10.1002/joc.2331>
- Vogel, R. M., Yaindl, C., & Walter, M. (2011). Nonstationarity: Flood magnification and recurrence reduction factors in the United States. *Journal of the American Water Resources Association*, 47(3), 464–474. <https://doi.org/10.1111/j.1752-1688.2011.00541.x>
- Wallace, J. M., & Gutzler, D. S. (1981). Teleconnections in the geopotential height field during the Northern Hemisphere winter. *Monthly Weather Review*, 109(4), 784–812. [https://doi.org/10.1175/1520-0493\(1981\)109<0784:TITGHP>2.0.CO;2](https://doi.org/10.1175/1520-0493(1981)109<0784:TITGHP>2.0.CO;2)
- Warnes, G. R., Bolker, B., & Lumley, T. (2020). *tools: Various R Programming Tools. R package version 3.8.2*. Retrieved from <https://CRAN.R-project.org/package=gtools>
- Wasko, C., Nathan, R., & Peel, M. C. (2020). Trends in global flood and streamflow timing based on local water year. *Water Resources Research*, 56(8), e2020WR027233. <https://doi.org/10.1029/2020WR027233>
- Wasko, C., Nathan, R., Stein, L., & O’Shea, D. (2021). Evidence of shorter more extreme rainfalls and increased flood variability under climate change. *Journal of Hydrology*, 603, 126994. <https://doi.org/10.1016/j.jhydrol.2021.126994>
- Wolman, M. G., & Miller, J. P. (1960). Magnitude and frequency of forces in geomorphic processes. *The Journal of Geology*, 68, 54–74. <https://doi.org/10.1086/626637>
- Ye, S., Li, H. Y., Leung, L. R., Guo, J., Ran, Q., Demissie, Y., & Sivapalan, M. (2017). Understanding flood seasonality and its temporal shifts within the contiguous United States. *Journal of Hydrometeorology*, 18(7), 1997–2009. <https://doi.org/10.1175/JHM-D-16-0207.1>